Entanglement generation from athermality

A. de Oliveira Junior [1,*] Jeongrak Son [2,*] Jakub Czartowski [3,4] and Nelly H. Y. Ng [2]

[1]*Center for Macroscopic Quantum States bigQ, Department of Physics,*
Technical University of Denmark, Fysikvej 307, 2800 Kgs. Lyngby, Denmark
[2]*School of Physical and Mathematical Sciences, Nanyang Technological University, Singapore 637371*
[3]*Doctoral School of Exact and Natural Sciences, Jagiellonian University, 30-348 Kraków, Poland*
[4]*Faculty of Physics, Astronomy and Applied Computer Science, Jagiellonian University, 30-348 Kraków, Poland*

We investigate the thermodynamic constraints on the pivotal task of entanglement generation using out-of-equilibrium states through a model-independent framework with minimal assumptions. We establish a necessary and sufficient condition for a thermal process to generate bipartite qubit entanglement, starting from an initially separable state. Consequently, we identify the set of system states that cannot be entangled, when no external work is invested. In the regime of infinite temperature, we analytically construct this set; while for finite temperature, we provide a simple criterion to verify whether any given initial state is or is not entangleable. Furthermore, we provide an explicit construction of the future thermal cone of entanglement—the set of entangled states that a given separable state can thermodynamically evolve to. We offer a detailed discussion on the properties of this cone, focusing on the interplay between entanglement and its volumetric properties. We conclude with several key remarks on the generation of entanglement beyond two-qubit systems, and discuss its dynamics in the presence of dissipation.

I. INTRODUCTION

Quantum dynamics and thermodynamics have been burgeoning areas of study, particularly in the domain of quantum information science [1–5]. Upon moving from the macroscopic world to the quantum realm, it is natural to ask how thermodynamics affects quantum information processing [6–9]. A thermodynamics-inspired paradigm for quantifying quantum correlations has led to the conclusion that one cannot extract the maximum work from an entangled state when it is shared by two separated parties [6,10]. Conversely, correlations shared between quantum systems allow for optimal work storage [9]. In tandem with these inquiries, the fundamental energetic limitations on creating both classical and quantum correlations have been thoroughly investigated [8,11–13], assuming closed system dynamics.

The task of correlation engineering becomes increasingly interesting in the more realistic scenario where quantum systems interact with a thermal environment, exchanging energy and entropy. Counterintuitively, it has been shown that entanglement can be induced by a single-mode heat environment [14] and that steady-state entanglement can be generated [15–18] even when no external agents are involved [19].

In particular, one can generate a maximally entangled steady state between two qubits deterministically using a third ancillary qubit [20]. These results suggest a paradigm shift where certain dissipative processes, rather than being detrimental to quantum correlations, might harness environment interactions for thermodynamically stable entanglement generation. As a result, a natural question arises: What are the thermodynamic limitations for quantum correlation and entanglement generation?

A powerful toolkit for answering this question is the resource-theoretic approach [21,22]. One may initially think that the entanglement resource theory of local operations and classical communication (LOCC) should be the relevant framework for the entanglement manipulation problem. However, LOCC operations are naturally motivated only after entanglement has been distributed; if one is instead at the preparation phase in a local laboratory, prior to entanglement distribution, then it is more reasonable to consider a resource theory that contains entangling operations. If entangling operations are allowed, the main limiting factor must come from quantum control and energetics [23–26], which leads us to the resource theory of quantum thermodynamics. This model-independent framework allows one to investigate general thermodynamic processes by relying solely on the assumptions of total energy conservation and thermality of environments. Its broad scope has allowed us to establish bounds on the size of the bath required for the thermalization of a many-body system [27], bridge the gap between Markovian and non-Markovian thermal processes [28,29], and uncover optimal heat-bath algorithmic cooling strategies [30], among other significant results (see Refs. [26,31] for recent reviews).

*These authors contributed equally to this work.

In this work, we systematically probe the capability of using thermal processes to generate entanglement when given access to some initial state. In the particular case of two qubits, we derive necessary and sufficient conditions for the existence of a thermal process that transforms a given separable initial state into a final state that is entangled. These conditions depend only on the energetic populations of the two-qubit system. A key insight that led to this finding, is the observation that a generic entangling strategy can be decomposed into two independent procedures: one that is explicitly achieved by open system dynamics (interaction with heat bath that results in changes of energetic population), and another closed unitary operation, i.e., an optimal rotation within the global energy subspace. The consistency of our results is confirmed by the problem addressed in Refs. [11,13], where the authors investigate two-qubit mixed states and determine unconstrained global unitary operations that generate maximal entanglement. We approach the considered problem with additional restrictions on the allowed operations, motivated by cornerstone findings on thermodynamic resource theories. To be specific, we assume that entangling operations must fall into the set of thermal operations [23,32].

Using the above framework we provide an explicit construction of the set of separable states that can become entangled. The degree of entanglement in this set can be assessed either by the volume of the set or by their negativity. In this regard, our results show that a Bell pair can always be thermodynamically produced at any temperature regime, provided that the system is initialized in its pure excited state. We also discuss the generation of entanglement in the presence of dissipation, examining the behavior of the volume of the future thermal cone of entanglement under Markovian thermal processes, and comparing it with the closed dynamics case. Finally, we offer some remarks on how our results can be extended to systems beyond two qubits.

The paper is organized as follows. We start by motivating how thermal resources can be used to generate entanglement in Sec. II, using an experimentally relevant example involving two spins interacting with a cavity mode. After this warmup, we set the scene in Sec. III by recalling the resource-theoretic approach to quantum thermodynamics. In Sec. IV, we rigorously define the main quantifiers used for entanglement generation under thermal operations in arbitrary dimensions. Section V focuses on the two-qubit system, and we derive necessary and sufficient conditions for entanglement preparation, and proceeds to quantify the entanglement generated and discuss its applicability. We discuss in Sec. VI how the task of entanglement generation changes for continuous-time thermal processes and high-dimensional systems, and conclude with an outlook in Sec. VII.

II. MOTIVATING EXAMPLES

Let us begin with a warmup example that gives a flavor of the main investigation. Consider two qubits A and B, with the former prepared in the ground state and the latter in the excited state. The joint state of the composite system is given by $\rho_{AB} = |01\rangle\langle 01|$. Furthermore, assume that each qubit is described by the Hamiltonian $H_0 = E|1\rangle\langle 1|$, the composite AB is described by a Hamiltonian $H = H_0 \otimes \mathbb{1} + \mathbb{1} \otimes H_0$.

This Hamiltonian gives rise to the degenerate energy subspace $\mathcal{V}_E = \text{span}\{|01\rangle, |10\rangle\}$, associated with energy E. Then any unitary acting nontrivially only on $\mathcal{V}_E$ is energy preserving, including

$$U = \frac{1}{\sqrt{2}}\begin{pmatrix} 1 & 1 \\ 1 & -1 \end{pmatrix} \oplus \mathbb{1}_{\mathcal{H}\setminus\mathcal{V}_E}, \tag{1}$$

that maps product states $|01\rangle$ and $|10\rangle$ into Bell states $|\phi^+\rangle$ and $|\phi^-\rangle$, where $|\phi^\pm\rangle = \frac{1}{\sqrt{2}}(|01\rangle \pm |10\rangle)$. In particular, when the initial state is either $|01\rangle$ or $|10\rangle$, this transformation can be implemented with Jaynes-Cummings interactions only [33]

$$H_{JC} = \sigma_{A(B)}^+ \otimes a_R + \sigma_{A(B)}^- \otimes a_R^\dagger, \tag{2}$$

albeit indirectly by introducing a mediating bosonic mode R [34]. We use the notation $\sigma^+ = |1\rangle\langle 0|$ and $\sigma^- = |0\rangle\langle 1|$ for each qubit A or B, while a_R and $a_R^\dagger$ are the annihilation and creation operators for the bosonic mode.

Suppose now that both qubits are prepared in the ground state, $\rho_{AB} = |00\rangle\langle 00|$. Then, it is impossible to entangle them using Eq. (1), or any other energy-preserving unitary acting on the composite AB, as ρ_{AB} has no support in $\mathcal{V}_E$. However, in the presence of a thermal bath, the populations of the composite system can be modified, thereby enabling the generation of entanglement. A simple yet experimentally relevant example illustrating this effect involves a two-step protocol. First, assume access to a bosonic mode with a resonant Hamiltonian $H_R = E a_R^\dagger a_R$, thermalized with respect to an inverse temperature β. Qubit B interacts with the bosonic mode for a finite time, which creates nonzero support of the composite state in $\mathcal{V}_E$. Second, apply the unitary given in Eq. (1). This two-step protocol transforms ρ_{AB} into

$$\sigma_{AB} = f(\beta E)|00\rangle\langle 00| + [1 - f(\beta E)]|\phi^+\rangle\langle \phi^+|. \tag{3}$$

The ground-state population $f(\beta E)$ depends on the interaction Hamiltonian and the duration of the interaction, in addition to the temperature and the energy gap. Let us assume that we apply Jaynes-Cummings interaction in Eq. (2) and optimize the time duration to minimize $f(\beta E)$. It turns out that this optimized quantity decreases monotonically as βE decreases. Hence, by additionally allowing the initial state $\rho_{AB} = |00\rangle\langle 00|$ to interact with a thermal bath, one can generate entangled states; higher amounts of entanglement can be observed at higher temperatures as well as with smaller energy gaps. The same protocol can be applied when both spins are excited. However, for this initial state, contrary to the previous example, $f(\beta E)$ is the smallest, and thus the final state is more entangled, when the ambient temperature is lower. In Fig. 1, we quantify the optimal amount of entanglement produced in these two cases, measured via the negativity, as a function of the inverse temperature of the bosonic mode.

In the above discussion, we have constructed specific thermal processes that precondition the composite state into entangleable ones, by using a simple bosonic mode and the Jaynes-Cummings interaction. A natural question follows: What is the ultimate bound of the entanglement generation, for the most generic, all-encompassing set of thermal processes?
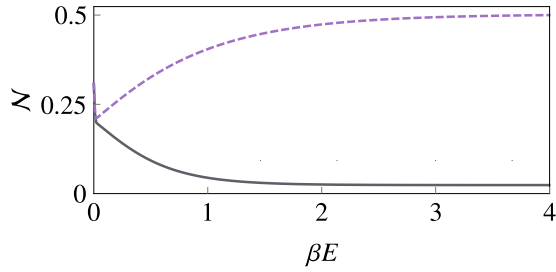
FIG. 1. Negativity as a function of βE. Preprocessing the spin system by coupling to a thermal bath opens up the possibility of generating entanglement through energy-preserving unitaries that encode the laws of thermodynamics. We plotted the maximal negativity [35] [defined in Eq. (31)] obtainable by a two-step process (i) transforming one of the spins via Jaynes-Cummings interaction with a thermal bosonic mode and (ii) applying the entangling unitary, Eq. (1). The x axis is the product of inverse environment temperature β and energy gap E. The black solid curve represents the resulting negativity from a state initially prepared in the ground state, while the purple dashed curve is that of the initially fully excited state.

III. SETTING THE SCENE

We investigate entanglement generation in an N-partite system whose initial state and the noninteracting Hamiltonian are given as

$$\rho \in \text{conv}\left(\bigotimes_{i=1}^{N} \rho_i\right) \quad \text{and} \quad H = \sum_{i=1}^{N} \mathbb{1}^{\otimes(i-1)} \otimes H_i \otimes \mathbb{1}^{\otimes(N-i)}. \tag{4}$$

The assumption that the Hamiltonian is noninteracting is natural, and excludes the trivial scenario of entangling simply via a fully thermalizing process. The Hilbert space of the composite system is denoted by $\mathcal{H} = \bigotimes_{i=1}^{N} \mathcal{H}_i$. The energy level structure creates a natural division of the full Hilbert space into energy-degenerate subspaces $\mathcal{V}_E$,

$$\mathcal{H} = \bigoplus_{E} \mathcal{V}_E, \tag{5}$$

where $\mathcal{V}_E = \text{span}\{|\psi\rangle \in \mathcal{H} : H|\psi\rangle = E|\psi\rangle\}$. Note that energy-preserving unitaries acting on $\mathcal{H}$ are those that can be written as $U = \bigoplus_E U_E$, where each unitary U_E acts on $\mathcal{V}_E$. In other words, they do not mix states from different energy subspaces—an essential feature for subsequent considerations.

A. Thermal operations

The multipartite system interacts with the thermal environment that is initialized in a Gibbs state

$$\gamma_{\mathsf{R}} = \frac{e^{-\beta H_{\mathsf{R}}}}{\text{Tr}(e^{-\beta H_{\mathsf{R}}})}, \tag{6}$$

with a Hamiltonian H_{R} and an inverse temperature β. We make minimal assumptions on the joint system-bath dynamics: the composite system is closed and thus evolves unitarily; in addition, this unitary evolution is energy preserving. Formally, this leads to a set of operations known as thermal

operations (TOs) [23], which transform the state ρ as follows:

$$\mathcal{E}(\rho) = \text{Tr}_{\mathsf{R}}[U(\rho \otimes \gamma_{\mathsf{R}})U^{\dagger}], \tag{7}$$

where U is a joint unitary that commutes with the total Hamiltonian of the system and the bath

$$[U, H \otimes \mathbb{1}_{\mathsf{R}} + \mathbb{1} \otimes H_{\mathsf{R}}] = 0, \tag{8}$$

and the environment Hamiltonian H_{R} can be chosen arbitrarily. Given that there are no further constraints on U, the system and the bath can develop arbitrarily strong correlations (including entanglement).

B. State transformation conditions

We focus on energy-incoherent states ρ, which means that each partition is (block) diagonal in the energy eigenbasis, resulting in an output state that is also (block) diagonal. Mathematically, the multipartite state ρ commutes with the Hamiltonian, i.e., $[\rho, H] = 0$. Under this assumption, the state ρ can be fully represented by a probability vector $\boldsymbol{p}$ consisting of the eigenvalues of ρ, which correspond to populations in the energy eigenbasis, $\rho = \sum_i p_i |E_i\rangle\langle E_i|$. We henceforth directly refer to $\boldsymbol{p} = (p_1, \ldots, p_d)$ as energy-incoherent states, which live within the probability simplex

$$\Delta_d = \left\{ \boldsymbol{p} = (p_1, \ldots, p_d) \in \mathbb{R}_{\geqslant 0}^d : \sum_i p_i = 1 \right\}. \tag{9}$$

Analogously, the thermal equilibrium state of the system, Eq. (6) with H_{R} replaced by H, can be represented by a vector of thermal populations, denoted as $\boldsymbol{\gamma}$.

When considering transformations between different energy-incoherent states under thermal operations, an important aspect of a state is its associated β order, a permutation which arranges populations, rescaled with respect to the Gibbs state, in a nonincreasing order.

Definition 1 (β ordering). Suppose that population vectors $\boldsymbol{p}$ and $\boldsymbol{\gamma}$, corresponding to a d-dimensional system state and its Gibbs state with respect to the ambient temperature $1/\beta$, are given. The β ordering of $\boldsymbol{p}$ is given as a permutation $\pi_{\boldsymbol{p}} \in \mathcal{S}_d$ of energy levels within the symmetric group $\mathcal{S}_d$, such that the elementwise ratio between $\boldsymbol{p}$ and $\boldsymbol{\gamma}$ is nonincreasing, i.e.,

$$\frac{p_{(\pi_p)i}}{\gamma_{(\pi_p)i}} \geqslant \frac{p_{(\pi_p)j}}{\gamma_{(\pi_p)j}}, \quad \text{for all} \quad i \leqslant j. \tag{10}$$

For simplicity, we also denote a β ordering π as a vector $\boldsymbol{\pi} = [\pi(1), \pi(2), \cdots, \pi(d)]$ in the rest of the paper. For the specific case of $d = 4$, we denote the β ordering (2,1,3,4) as $\boldsymbol{\pi}^{\star}$, since it plays a special role in entanglement generation, which will become clear in Sec. IV (Theorem 1).

Finally, the set of states $\mathcal{T}_+(\boldsymbol{p})$ that can be achieved via thermal operations from a given initial state $\boldsymbol{p}$ is called the future thermal cone [36,37]. This set is a convex polytope comprising at most $d!$ extreme points, each corresponding to different β orderings $\boldsymbol{\pi}$ [36,37]. Mathematically, it is represented by:

$$\mathcal{T}_+(\boldsymbol{p}) = \text{conv}[\boldsymbol{p}^{\boldsymbol{\pi}}, \boldsymbol{\pi} \in \mathcal{S}_d], \tag{11}$$

where $\boldsymbol{p}^{\boldsymbol{\pi}}$ are extreme points characterized by thermomajorization [38] (see Lemma 2, Appendix A). Again, for $d = 4$,

we denote the extreme point corresponding to the ordering $\boldsymbol{\pi}^\star$ as $\boldsymbol{p}^\star$.

Although not explicitly stated, it is important to mention that the existence of a thermal operation that induces the transition between incoherent states $\boldsymbol{p} \rightarrow \boldsymbol{p}'$ is equivalent to the existence of a Gibbs-preserving (GP) stochastic matrix mapping between these states [23]. Therefore, when studying the thermodynamic interconversion problem between block diagonal states, one can focus on stochastic matrices and probability vectors instead of CPTP maps and density matrices. Nonetheless, our forthcoming discussion will primarily center on the concept of thermal cones, rather than on GP matrices or thermal operations.

IV. ENTANGELABILITY UNDER THERMAL OPERATIONS

In this section, we introduce the main definitions that will enable us to derive the necessary and sufficient conditions for entangling a separable state under thermal operations. At first glance, this might appear abstract due to its generality, but these notions will be applied to a specific case in Sec. V.

We begin by defining a subset of unitary operations that preserve the energy of the system and keep the energy level structure intact. Note that this is motivated by capturing the thermodynamic constraints in producing entanglement when the system is closed, i.e., when the unitary dynamics satisfy energy conservation. We refer to this subset as energy subspace unitaries, denoted by $\mathcal{U}_{\text{subs}}$. Formally, this set is given by

$$\mathcal{U}_{\text{subs}} = \left\{ U_{\text{subs}} = \bigoplus_E U_E \right\}, \tag{12}$$

where U_E acts on $\mathcal{V}_E$ subspace of definite energy E. Consequently, any unitary operation from this set is an admissible operation within the framework of thermal operations.

Let us note that the existence of energy-degenerate subspaces containing entangled states is necessary for our approach to entanglement generation using thermal operations. If there are no such subspaces, all entangled states require coherence between eigenstates corresponding to different energies, which cannot be generated via thermal operations [39]. Alternatively, one can consider slightly different set of operations that can create the coherence, such as Gibbs-preserving operations [40] or quantify the entanglement generation cost by incorporating batteries in the picture.

Next, we introduce an entanglement measure $\mathcal{M}$, which is non-negative for all separable states, $\mathcal{M}(\rho_{\text{sep}}) \geqslant 0$. One such entanglement measure which we focus on is derived from the famous Horodecki-Peres positive partial transpose (PPT) criterion [41,42], which states that separable states have positive partial transpose, $\rho^{T_A} \geqslant 0$; using this, we define $\mathcal{M}(\rho) := \min_{|\psi\rangle}\langle\psi|\rho^{T_A}|\psi\rangle = \lambda_-$ as the minimal eigenvalue of the partial transpose. Therefore, the quantity

$$f(\boldsymbol{p}) := \min_{U \in \mathcal{U}_{\text{subs}}} \mathcal{M}(U\rho U^\dagger) \tag{13}$$

is a good witness for the thermodynamic capacity of creating entanglement from $\boldsymbol{p}$ via closed, energy-conserving system dynamics.

Definition 2 [Subspace (non)entangleable set]. Given a state $\boldsymbol{p} \in \Delta_d$, the subspace nonentangleable set is defined as the set of states that remain PPT under subspace rotations, i.e.,

$$\mathbb{NE} := \{\boldsymbol{p} \mid f(\boldsymbol{p}) \geqslant 0\}. \tag{14}$$

The function f acts as an entanglement witness, i.e., $f(\boldsymbol{p}) \leqslant 0$ implies the possibility of creating entanglement. Furthermore, the subspace entangleable set is defined as the complement of $\mathbb{NE}$, i.e., $\mathbb{E} := \Delta_d \backslash \mathbb{NE}$.

This definition can be extended by employing multiple entanglement measures $\mathcal{M}_1, \ldots, \mathcal{M}_M$, resulting in multiple witnesses $f_1, \ldots, f_M$, and requiring that all these functions yield positive values.

It is important to note that states in the set $\mathbb{E}$ are entangleable even when neither heat or work exchange are allowed. Notably, when thermal resources are available, i.e., under thermal operations, the set of entangleable states expand.

Definition 3 (Future thermal cone of entanglement). The future thermal cone of entanglement of a state $\boldsymbol{p}$ is defined as

$$\mathcal{T}_+^{\text{ENT}}(\boldsymbol{p}) := \{\boldsymbol{q} \mid f(\boldsymbol{q}) < 0, \ \boldsymbol{q} \in \mathcal{T}_+(\boldsymbol{p})\} = \mathcal{T}_+(\boldsymbol{p}) \cap \mathbb{E}. \tag{15}$$

Now we introduce the primary object of this paper: the set of states that cannot become entangled under thermal operations.

Definition 4 (Thermally nonentangleable set). Given the ambient temperature β^{-1}, the thermally nonentangleable set is defined as

$$\mathbb{TNE}(\beta) = \left\{ \boldsymbol{p} \mid \min_{\boldsymbol{q} \in \mathcal{T}_+(\boldsymbol{p})} f(\boldsymbol{q}) \geqslant 0 \right\}, \tag{16}$$

with the entanglement measure $\mathcal{M}$. Analogous to $\mathbb{E}$, we also define the set of thermally entangleable states $\mathbb{TE}(\beta) := \Delta_d \backslash \mathbb{TNE}(\beta)$.

By definition, $\boldsymbol{p}$ is thermally nonentangleable if and only if its future cone of entanglement is empty, i.e.,

$$\boldsymbol{p} \notin \mathbb{TNE}(\beta) \iff \mathcal{T}_+^{\text{ENT}}(\boldsymbol{p}) = \varnothing. \tag{17}$$

We can then characterize $\mathbb{TNE}(\beta)$ with the following proposition. Hereafter, we drop the explicit dependence on β in $\mathbb{TNE}$ and $\mathbb{TE}$ when there is no concern for confusion.

Proposition 1 (Thermally nonentangleable set). Suppose that the entanglement measure $\mathcal{M}$ is a concave function. Then the set $\mathbb{TNE}$ can be written as

$$\mathbb{TNE} = \{\boldsymbol{p} \mid \forall_\pi f(\boldsymbol{p}_\pi) \geqslant 0\}. \tag{18}$$

When $\beta E = 0$, the above expression simplifies to

$$\mathbb{TNE} = \bigcap_{\pi \in \mathcal{S}_d} \{\boldsymbol{p} \mid f(\Pi\boldsymbol{p}) \geqslant 0\} =: \bigcap_{\pi \in \mathcal{S}_d} \Omega_\pi, \tag{19}$$

where Π represents a permutation matrix corresponding to $\pi \in \mathcal{S}_d$; in particular, for $\pi = \text{id}$ we have $\Omega_{\text{id}} = \mathbb{NE}$.

Definition 3 also allows us to quantify the entanglement generation power using geometric measures. The volume of the future thermal cone of entanglement can gauge how useful an initial state is for producing entangled states. Given a state $\boldsymbol{p}$, this quantity is defined as

$$\mathbf{V}_{\text{TO}}^{\text{ENT}}(\boldsymbol{p}) := \frac{V[\mathcal{T}_+^{\text{ENT}}(\boldsymbol{p})]}{V(\Delta_d)}, \tag{20}$$

where V is the volume measured using the Euclidean metric. Likewise, the volume of (non)entangleable sets, defined in Definitions 2 and 4, are denoted as

$$\mathbf{V}_{\mathbb{X}} := \frac{V(\mathbb{X})}{V(\Delta_d)}, \quad \mathbb{X} = \mathbb{NE}, \ \mathbb{E}, \ \mathbb{TNE}. \tag{21}$$

V. TWO-QUBIT SYSTEMS

Let us now apply the general framework we developed to a specific scenario: two-qubit entanglement. In this section, we find an efficient criterion for determining whether a two-qubit state $\boldsymbol{p}$ is thermally nonentangleable, which only checks if $\boldsymbol{p}^\star$ is subspace nonentangleable. We also study the geometry of the future thermal cone of entanglement and the thermally nonentangleable set for different ambient temperatures.

A. Subspace entangleable set for two qubits

Assume that Alice and Bob share a pair of qubits that are initially prepared in a separable state ρ_{AB}. Each of them is described by a local Hamiltonian $H_{\mathsf{A}} = H_{\mathsf{B}} = E|1\rangle\langle 1|$, and they are allowed to interact with a single heat bath via thermal operations. If there exists a thermal operation that maps ρ_{AB} to σ_{AB}, where $[\rho_{\mathsf{AB}}, H] = 0$ and $[\sigma_{\mathsf{AB}}, H] = 0$, then σ_{AB} can be expressed as

$$\sigma_{\mathsf{AB}} = q_1|00\rangle\langle 00| + q_2|\psi\rangle\langle\psi| + q_3|\psi_\perp\rangle\langle\psi_\perp| + q_4|11\rangle\langle 11|, \tag{22}$$

where $|\psi\rangle, |\psi^\perp\rangle \in \mathcal{V}_E$ and $\langle\psi|\psi^\perp\rangle = 0$. This observation follows from the fact that one can freely rotate the populations within the degenerate energy subspace. The unitary that connects $|\psi\rangle = U|10\rangle$ and $|\psi_\perp\rangle = U|01\rangle$ can be written with two parameters $\theta, \phi \in [0, 2\pi]$

$$U = \begin{pmatrix} \cos\theta & \sin\theta e^{i\phi} \\ -\sin\theta e^{-i\phi} & \cos\theta \end{pmatrix} \oplus \mathbb{1}_{\mathcal{H}\backslash\mathcal{V}_E}, \tag{23}$$

apart from an irrelevant phase factor, global to $\mathcal{V}_E$. Then the final state σ reads

$$\sigma = \begin{pmatrix} q_1 & 0 & 0 & 0 \\ 0 & q_2\cos^2\theta + q_3\sin^2\theta & \frac{(q_3-q_2)}{2}\sin 2\theta e^{i\phi} & 0 \\ 0 & \frac{(q_3-q_2)}{2}\sin 2\theta e^{-i\phi} & q_2\sin^2\theta + q_3\cos^2\theta & 0 \\ 0 & 0 & 0 & q_4 \end{pmatrix}. \tag{24}$$

For a two-qubit system, separability can be fully determined by the positive partial transposition (PPT) criterion [41,42]. When the partial transposition is applied to the state σ in Eq. (24), its smallest eigenvalue is

$$\lambda_- = \frac{1}{2}\left[(q_1 + q_4) - \sqrt{[(q_2 - q_3)^2\sin^2 2\theta + (q_1 - q_4)^2]}\right], \tag{25}$$

which is minimized when $\sin^2 2\theta = 1$.[1] Thus, λ_- can become negative if and only if

$$4q_1q_4 < (q_2 - q_3)^2. \tag{26}$$

In other words, a state with population vector $\boldsymbol{q} = (q_1, q_2, q_3, q_4)$ is subspace entangleable if and only

---

[1] This minimum value coincides with the case where we diagonalize the energy degenerate subspace in Bell basis, i.e., $|\psi\rangle, |\psi_\perp\rangle = |\Psi^\pm\rangle$.

(a) $(0,0,0,1)$

$(0,0,1,0)$
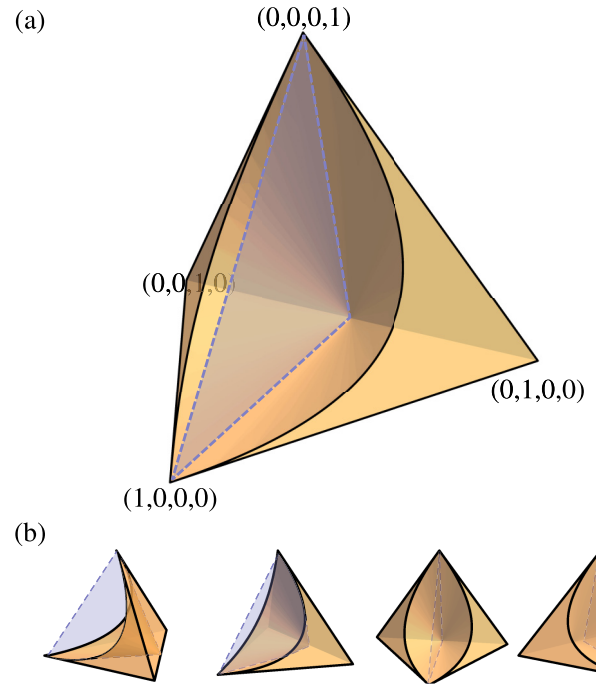
$(0,1,0,0)$

$(1,0,0,0)$

(b)

FIG. 2. Subspace entangleable set $\mathbb{E}$. Geometry of the set of states that can get entangled via energy-preserving unitaries acting on the degenerate energy subspace. Note that the set $\mathbb{E}$ consists of two disjoints sets each on the opposite side of the plane $p_2 = p_3$ colored in blue.

if Eq. (26) is true. We will refer to this inequality as the entanglement constraint or criterion. In addition, we define an associated entanglement measure

$$f(\boldsymbol{q}) := 4q_1q_4 - (q_2 - q_3)^2, \tag{27}$$

which detects entanglement whenever $f(\boldsymbol{q}) < 0$.

Figure 2 depicts the subspace entangleable set $\mathbb{E}$ (see Fig. 11 in Appendix B for its complement $\mathbb{NE}$). States in $\mathbb{E}$ can become entangled by some energy-preserving unitary of the form Eq. (23).

The sets $\mathbb{NE}$ and $\mathbb{E}$ are independent of the ambient temperature and their volume can be calculated by numerical methods or direct integration. Remarkably, the normalized volume of $\mathbb{E}$ is approximately $\mathbf{V}_{\mathbb{E}} \approx 21/62$; much less than half of the states in Δ_4 are subspace entangleable. In contrast, as we note in Sec. V C, the future thermal cone of entanglement of the highest excited state $\boldsymbol{p} = (0, 0, 0, 1)$ is precisely $\mathbb{E}$, as this state can achieve any other state in the probability simplex, regardless of the ambient temperature. Hence, the full volume $\mathbf{V}_{\mathbb{E}}$ can be achieved via thermal operations. Furthermore, we prove the convexity of the subspace nonentangleable set, find its extreme points, and identify a continuous family of boundary points (Appendix B).

B. Thermally entangleable states

We now construct the set of states that can generate entanglement with the help of a thermal environment. In the simple case of $\beta E = 0$, its complement, the set of thermally nonentangleable states $\mathbb{TNE}$, can be immediately constructed
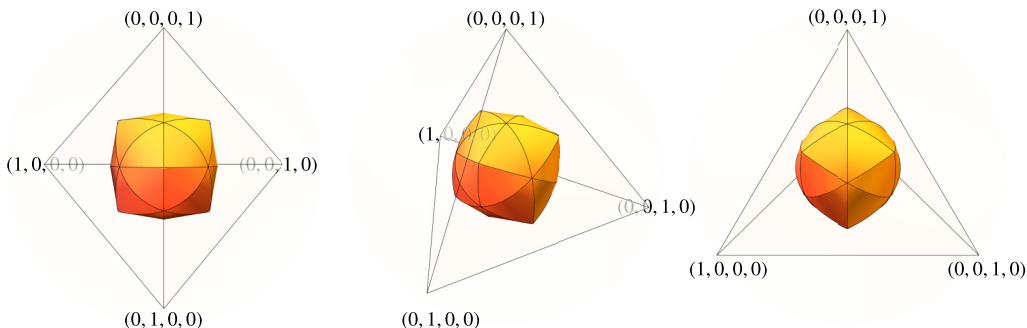
FIG. 3. Thermally nonentangleable states $\mathbb{TNE}$ for $\beta E = 0$. States that belong to the colored geometrical shape cannot get entangled under thermal operations when $\beta E = 0$.

from Proposition 1. The resulting set is convex and occupies approximately one third of the probability simplex (see Fig. 3). However, the structure of this set becomes more intricate when $\beta E \neq 0$. Nevertheless, we simplify the problem by showing that the task of determining whether $\boldsymbol{p} \in \mathbb{TNE}$, defined by Eq. (16) as including a nontrivial minimization, is reduced to verifying if $\boldsymbol{p}^{\star} \in \mathbb{NE}$, which only requires checking a single inequality $f(\boldsymbol{p}^{\star}) \geqslant 0$.

Theorem 1 (Criterion for determining $\boldsymbol{p} \in \mathbb{TE}$). Let $\boldsymbol{p}$ be a two-qubit state in $\mathbb{TE}$. Then $\boldsymbol{p}^{\star}$, the extreme point of $\mathcal{T}_{+}(\boldsymbol{p})$ corresponding to the β ordering $\boldsymbol{\pi}^{\star} = (2, 1, 3, 4)$, is in $\mathbb{E}$.

The full proof is detailed in Appendix C, and consists in two main steps. First, we identify $\boldsymbol{\pi}^{\star}$ as a special β ordering for subspace entangleability: whenever $\boldsymbol{p} \in \mathbb{TNE}$, there exists a state $\boldsymbol{q} \in \mathcal{T}_{+}^{\mathrm{ENT}}(\boldsymbol{p})$ with the ordering $\boldsymbol{\pi}^{\star}$ (Theorem 6). Next, we use a geometric argument (Proposition 7) to prove that whenever there exists such $\boldsymbol{q}$, the extreme point $\boldsymbol{p}^{\star}$ is also subspace entangleable, i.e. $\boldsymbol{p}^{\star} \in \mathcal{T}_{+}^{\mathrm{ENT}}(\boldsymbol{p})$. It is, however, important to note that Theorem 1 does not imply that the minimum of $f(\boldsymbol{q})$ over $\boldsymbol{q} \in \mathcal{T}_{+}(\boldsymbol{p})$ is always achieved when $\boldsymbol{q} = \boldsymbol{p}^{\star}$. For a simple counterexample, consider a state $\boldsymbol{p} = (\epsilon, 1 - \epsilon - \epsilon^2, 0, \epsilon^2)$ with $\epsilon \ll e^{-2\beta E}$. The state $\boldsymbol{p}$ has a β ordering $(2, 1, 4, 3)$, yet a smaller f value $f(\boldsymbol{p}) < f(\boldsymbol{p}^{\star})$ compared to $\boldsymbol{p}^{\star}$.

The interplay between the temperature β^{-1} of the immediate environment and the ability to entangle a system manifests in Theorem 1 through the β ordering. We numerically quantify the volume of the thermally nonentangleable state set $\mathbb{TNE}$ in Fig. 4. For any finite temperature regime $\beta > 0$, determining all states that are thermally nonentangleable is not straightforward. We devise a computationally efficient algorithm, using Theorem 1 and the vacuum-packing-inspired procedure, that approximates $\mathbb{TNE}$ for given β:

(1) Generate a regular grid on the surface of the probability simplex Δ_3.

(2) Select a point $\boldsymbol{p}_o^{(0)}$ from the grid and the Gibbs state $\boldsymbol{p}_i^{(0)} = \boldsymbol{\gamma}$. With this choice, we are guaranteed to have $\boldsymbol{p}_o^{(0)} \in \mathbb{TE}$ and $\boldsymbol{p}_i^{(0)} \in \mathbb{TNE}$.[2]

(3) In the jth step of the procedure we define midpoint $\boldsymbol{p}_m^{(j)} = \frac{1}{2}(\boldsymbol{p}_i^{(j)} + \boldsymbol{p}_o^{(j)})$ and, based on Theorem 1, decide

whether $\boldsymbol{p}_m^{(j)}$ is an element from the nonentangleable set. If $\boldsymbol{p}_m^{(j)} \in \mathbb{TNE}$, then $\boldsymbol{p}_i^{(j+1)} = \boldsymbol{p}_m^{(j)}$; else $\boldsymbol{p}_o^{(j+1)} = \boldsymbol{p}_m^{(j)}$.

(4) Repeat the bisection step $n = 30$ times, achieving the precision $\|\boldsymbol{p}_i^{(n)} - \boldsymbol{p}_o^{(n)}\| \approx 10^{-9} \|\boldsymbol{p}_i^{(0)} - \boldsymbol{p}_o^{(0)}\|$.

(5) Add the point $\boldsymbol{p}_m^{(n)}$ to the approximate set $\widetilde{\mathbb{TNE}}$.

(6) Repeat steps (ii)–(v) for all the grid points.

The convex hull of the final set $\mathrm{conv}(\widetilde{\mathbb{TNE}})$ is a good approximation of the actual nonentangleable set $\mathbb{TNE}$. The numerical result in Fig. 4 exhibits a monotonic behavior, indicating that low temperatures enhance entangleability. Indeed, this outcome is intuitively expected. Thermal processes permit the local bypassing of strict energy preservation, thereby offering advantage in terms of entanglement generation. Yet, thermal noise inevitably accompanies thermal processes, impacting the amount of achievable entanglement. The negative impact of thermal noise is anticipated to be minimized at lower environmental temperatures. We confirm this first by observing that the set of non-entangleable states $\mathbb{TNE}$ vanishes at the zero temperature limit $\beta \to \infty$. Moreover, we can make a more rigorous observation.

Lemma 1. The set $\mathbb{TNE}(\infty) = \{(1, 0, 0, 0)\}$, i.e., it contains only the ground state.
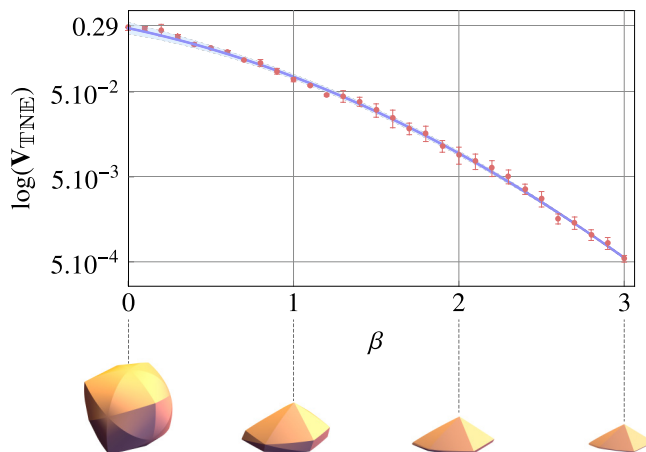

FIG. 4. Optimal entanglement generation regime. The top plot illustrates the approximated log volume of the set of states that cannot become entangled, as a function of β. The bottom plot demonstrates how the geometry of this set changes at specific values of β.

---

[2]Except for a single case $\boldsymbol{p}_o^{(0)} = \frac{1}{1 + 2e^{-\beta E}}(1, e^{-\beta E}, e^{-\beta E}, 0)$.

Proof. Given any other initial state, it is possible to thermalize one of the subsystems; in the zero-temperature limit ($\beta \to \infty$), this transforms a state $\boldsymbol{p} = (p_1, p_2, p_3, p_4)$ into $\boldsymbol{q} = (p_1 + p_3, p_2 + p_4, 0, 0)$ or $(p_1 + p_2, p_3 + p_4, 0, 0)$. However, in this specific scenario, it is sufficient to assume entanglement because the last two levels are empty while the second level is populated. Consequently, f always becomes negative. Thus, for any state $\boldsymbol{p} \neq (1, 0, 0, 0)$, the final state $\boldsymbol{q}$ is subspace entangleable, i.e., $\boldsymbol{p} \in \mathbb{TE}$. ∎

One may be tempted to view the ground state $(1,0,0,0)$ then as useless for entanglement generation; however, this is not true. In particular, the ground state becomes thermally entangleable whenever $\beta^{-1} \neq 0$: one can thermalize one of the subsystems to obtain $\boldsymbol{q} = \frac{1}{1+e^{-\beta E}}(1, e^{-\beta E}, 0, 0)$, which is subspace entangleable. What is observed is that as long as there is a certain amount of athermality in the initial state (with respect to environment temperature), we can often trade it for some amount of entanglement.

Given the above, it is then intuitive to see that given an initial state $\boldsymbol{p}$, the range of environmental temperature that allows for entanglement generation is very much state dependent. In particular, we are able to identify critical inverse temperatures β_C, at which a state $\boldsymbol{p}$ starts to become thermally (non)entangleable. In fact, we show that β_C, if exists, can be directly calculated for any state by employing Theorem 1 alongside the entanglement constraint in Eq. (26). Interestingly, for some states two critical temperatures $\beta_{C_1} < \beta_{C_2}$ exist and the state becomes entangleable when $\beta < \beta_{C_1}$ or $\beta > \beta_{C_2}$. A particularly clear analysis can be done when the initial state themselves are thermal, having a temperature $\beta_S \neq \beta$ in principle different from the ambient temperature. We report the conclusions here, while directing the curious reader to the full calculation in Appendix D.

Thermal initial states are written as

$$\boldsymbol{p} = \frac{1}{Z_S}\big(1, e^{-\beta_S E}, e^{-\beta_S E}, e^{-2\beta_S E}\big), \tag{28}$$

where $Z_S = (1 + e^{-\beta_S E})^2$. When the system is colder than the environment, $\beta_S > \beta$, the β ordering of the state is $(1,2,3,4)$. Finding the explicit form of the extreme point $\boldsymbol{p}^\star$ and solving $f(\boldsymbol{p}^\star) = 0$, we may obtain the critical temperature

$$\beta_{C_1} \equiv \beta_S - E^{-1} \log\big[1 + 2e^{-\beta_S E}(\sqrt{e^{2\beta_S E} + 1} - 1)\big]. \tag{29}$$

Whenever the ambient temperature β^{-1} is higher than the critical temperature $\beta_{C_1}^{-1}$, the thermal state $\boldsymbol{p}$ becomes thermally entangleable. We can obtain a simple approximation $\beta_{C_1} \simeq \beta_S - E^{-1} \log 3$ of Eq. (29) up to the zeroth order of $e^{-\beta_S E}$ in the low system temperature limit $\beta_S E \gg 1$.

On the other hand, when the system is hotter than its surrounding, i.e. $\beta_S < \beta$, the critical temperature can be obtained from a quartic equation and we do not have an explicit formula for it. However, in the same limit $\beta_S E \gg 1$, we can approximate $\beta_{C_2} \simeq \beta_S + E^{-1} \log 3$. In other words, if

$$|\beta_S - \beta| \geqslant E^{-1} \log 3, \tag{30}$$

then we may operate such a thermal machine to generate entanglement. See Fig. 5 for the numerical values of the critical temperatures, which clearly displays the validity of our approximation $\beta_C \simeq \beta_S \pm E^{-1} \log 3$. As mentioned
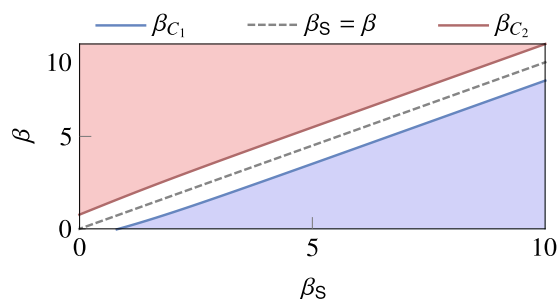

FIG. 5. Thermal state and entangleability. Critical temperatures of an environment for thermal initial states, where the qubit energy gap is set to $E = 1$. The x axis indicates the inverse temperature β_S of the initial state and the y axis marks the ambient inverse temperature β. If the pair (β_S, β) is in either blue or red shaded region, the thermal initial state is entangleable. The blue and red lines mark the hot critical (inverse) temperature and cold critical (inverse temperature) for the environment to make the thermal initial state entangleable.

earlier, the temperature difference between the system and the environment is a resource for entanglement generation, as it is for many other thermodynamic tasks. This process can be conceptualized as a type of heat engine, which aims not to output work, but entanglement. For instance, consider a three-stroke thermal-entanglement engine whose working substance is a two-qubit system. This engine operates between an ambient bath at temperature β^{-1} and a working bath with temperature $\beta_W^{-1} : |\beta_W^{-1} - \beta_C^{-1}| > 0$. The cycle proceeds as follows: (i) the two-qubit system thermalizes with the working bath, reaching equilibrium state at the working bath's temperature β_W^{-1}, which corresponds to acquiring the initial athermality. (ii) The system is then brought into contact with the ambient bath, which is at temperature β^{-1} providing the underlying free thermal operations. During this stage, entanglement is generated within the two-qubit system. To close the cycle (iii) the generated entanglement is used, and the system is returned to its initial state, which is energy incoherent. Observe that this cycle cannot generate entanglement if the thermal operations are replaced by energy-preserving unitaries. The possibility of heat exchange with the ambient bath in (ii) is the critical factor that allows the entanglement generation from athermality.

C. Quantifiers for achievable entanglement under thermal operations

In the previous sections, we focused on determining whether a state is entangleable or not using thermal resources. Here, we are additionally interested in the extent of entanglement that thermal operations can produce, and how this varies across different temperature regimes. Two figures of merit can be used to quantify this extent: the thermal volume of entanglement, $\mathbf{V}_{\text{TO}}^{\text{ENT}}(\boldsymbol{p})$ as defined in Eq. (20) and the maximum negativity [35] that the initial state can produce. In particular, the thermal volume of entanglement is a thermodynamic monotone, in other words, $\mathbf{V}_{\text{TO}}^{\text{ENT}}(\boldsymbol{p}) \geqslant \mathbf{V}_{\text{TO}}^{\text{ENT}}(\boldsymbol{q})$ for all $\boldsymbol{q} \in \mathcal{T}_+(\boldsymbol{p})$. Further insights on this quantity can be developed by considering the geometry of the future thermal cone of entanglement $\mathcal{T}_+^{\text{ENT}}(\boldsymbol{p})$. Recall in Definition 3, $\mathcal{T}_+^{\text{ENT}}(\boldsymbol{p})$ is the intersection of two sets: $\mathbb{E}$ and $\mathcal{T}_+(\boldsymbol{p})$. We also
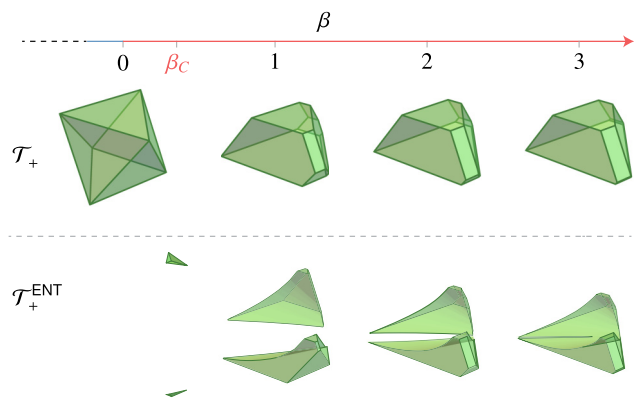
FIG. 6. Regions of entanglement. The evolution of the future and entanglement thermal cones as a function of β reveals interesting behavior. For a bipartite product state $\boldsymbol{p} = (0.5, 0.5) \otimes (0.24, 0.76)$ with an identical energy gap $E = 1$, we observe that at $\beta = 0$, the state cannot be entangled via thermal operations. However, for $\beta \geqslant \beta_C \approx 0.21$, the state becomes entangleable. As β increases, the two disjoint parts of $\mathcal{T}^{\text{ENT}}(\boldsymbol{p})$ become closer, until at $\beta \to \infty$, they are separated only by a plane $p_2 = p_3$.

know that $\mathbb{E}$ is nonconvex and not connected, hence $\mathcal{T}_+^{\text{ENT}}(\boldsymbol{p})$ is also nonconvex and not connected (see bottom panel of Fig. 6). However, as the temperature decreases, two disjoint parts grow in sizes and approach each other, becoming almost connected; this is a natural consequence of the future thermal cone approaching the plane $p_4 = 0$, which is on the boundary of $\mathbb{E}$.

The change in volume $\mathbf{V}_{\text{TO}}^{\text{ENT}}(\boldsymbol{p})$ with respect to β is, however, heavily dependent on the initial state. To see this, consider the energy eigenstates, i.e., four vertices of the probability simplex Δ_4 as described explicitly in the caption of Fig. 7. For the ground state $\boldsymbol{p}_1$, $\mathbf{V}_{\text{TO}}^{\text{ENT}}(\boldsymbol{p}_1)$ decreases with β (black solid curve, top panel of Fig. 7), because the future thermal cone $\mathcal{T}_+(\boldsymbol{p}_1)$ shrinks as the Gibbs state γ approaches the ground state as β increases. On the other hand, for the maximally excited state $\boldsymbol{p}_4$, $\mathcal{T}_+(\boldsymbol{p}_4)$ remains constant (red dot curve, top panel of Fig. 7), since the future thermal cone encompasses the entire probability simplex, regardless of the ambient temperature. In this case, the future thermal cone of entanglement is precisely $\mathbb{E}$. Finally, for both $\boldsymbol{p}_2$ and $\boldsymbol{p}_3$, the thermal volume of entanglement decreases with β, albeit slower than that of $\boldsymbol{p}_1$.

The second figure of merit is negativity [35],

$$\mathcal{N}(\rho) = \frac{\|\rho^{T_A}\|_1 - 1}{2} = \sum_i \frac{|\lambda_i| - \lambda_i}{2}, \tag{31}$$

where λ_i represents all the eigenvalues of ρ^{T_A}. Equivalently, $\mathcal{N}(\rho) = \sum_j |\lambda_j^-|$, where λ_j^- are negative eigenvalues of ρ^{T_A}. Therefore, if the system is qubit-qubit or qubit-qutrit, nonzero negativity is necessary and sufficient for the state being entangled; for any larger systems, there exist entangled states with zero negativity [43,44]. In the qubit-qubit system we are examining, given a population vector $\boldsymbol{q} = \text{eig}(\sigma)$, the maximal negativity can be obtained from Eq. (25) as

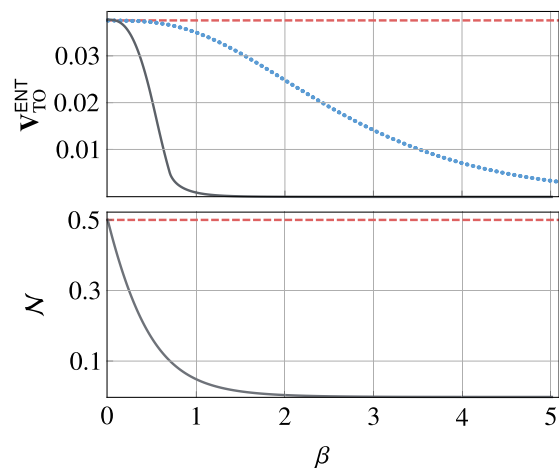$$\mathcal{N}(\sigma) = \frac{1}{2}[\sqrt{(q_1 - q_4)^2 + (q_2 - q_3)^2} - (q_1 + q_4)], \tag{32}$$

FIG. 7. Volume and negativity as a function of β. For all sharp states $\boldsymbol{p}_1 = (1, 0, 0, 0)$, $\boldsymbol{p}_2 = (0, 1, 0, 0)$, $\boldsymbol{p}_3 = (0, 0, 1, 0)$, and $\boldsymbol{p}_4 = (0, 0, 0, 1)$, we plot the thermal volume of entanglement (top), and the largest negativity as a function of the inverse temperature. Among all states, two are distinct: when both qubits start in the excited state $\boldsymbol{p}_4$ and when they start in the ground state (black solid curve) $\boldsymbol{p}_1$. Any other permutation of the initial state characterizes a different active state, and their volume is represented by the blue dotted curve on the top panel. Note that this plot also represents the normalized volume of subspace entangleable states, since the thermal cone of $\boldsymbol{p}_4$ is the full set space. Moreover, although the maximum achievable negativity of $\boldsymbol{p}_4$ is the same as, e.g., $(0, 1, 0, 0)$, it is much more powerful in terms of state preparation, which can be useful since entanglement is in general irreversibly manipulated. In the bottom panel, the maximum negativity of these states coincides with the maximally active state.

when $f(\boldsymbol{q}) < 0$, which has also been expected from Ref. [11] in a different context. Observe that Eq. (32) is related to Eq. (27) via

$$\mathcal{N}(\sigma) = \frac{1}{2}[\sqrt{(q_1 + q_4)^2 - f(\boldsymbol{q})} - (q_1 + q_4)], \tag{33}$$

and monotonically decreases as $f(\boldsymbol{q})$ increases. For $f(\boldsymbol{q}) \geqslant 0$, the negativity is always zero.

The maximum negativity over all probability simplex Δ_4 occurs when $\boldsymbol{q} = (0, 1, 0, 0)$ or $\boldsymbol{q} = (0, 0, 1, 0)$ and the corresponding state are the Bell states. If the system is initially in one of the four vertices of Δ_4, it is possible to prepare Bell states via thermal operations when $\beta = 0$. However, as $\beta \geqslant 0$, the ground state $\boldsymbol{p}_1$ loses its ability to produce a Bell state, while three other pure states remain capable. The maximum negativity that $\boldsymbol{p}_1$ can produce decreases as β increases.

As argued, maximum negativity is only reachable for very specific initial states. The natural question is how much negativity can be produced via thermal operations for general states. While the answer to this question depends heavily on the specific state under consideration, one can gain a general understanding by visualizing the degree of negativity generated by states that lie in the subspace entangleable and thermally entangleable sets. Figure 8(a), shows the maximal attainable negativity evaluated for all points in $\mathbb{E}$. Specifically, we consider different slices of the probability simplex, each having fixed p_1. This approach allows us to visualize the distribution and intensity of attainable negativity across
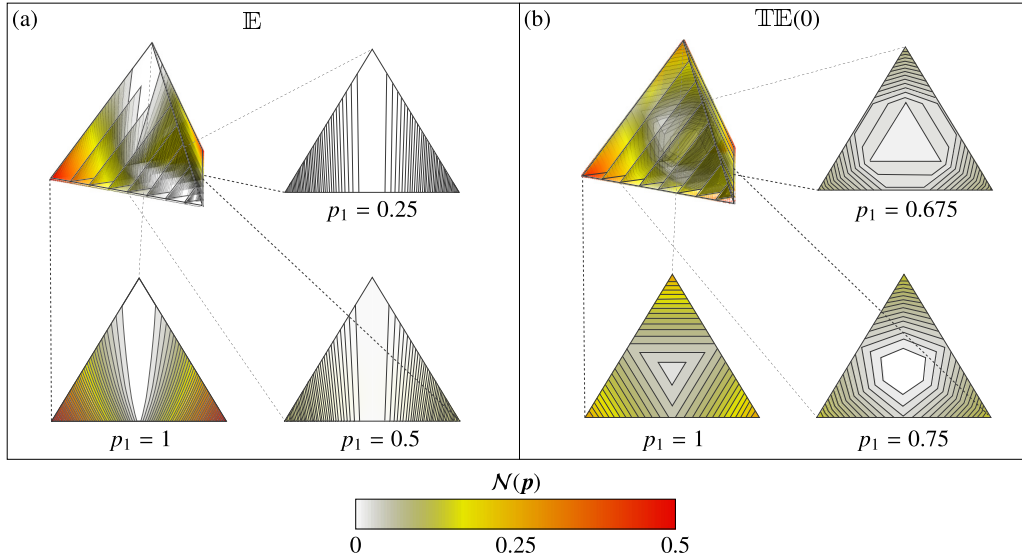
FIG. 8. Quantifying entanglement generation via thermal operations. The degree of negativity produced under energy-preserving unitaries and thermal operations can be visualized by slicing the entangleable and thermally entangleable sets and computing their maximal negativity. For two qubits with populations $\boldsymbol{p} = (p_1, p_2, p_3, p_4)$, we observe a high level of negativity in (a) subspace entangleable set and (b) thermally entangleable set for $\beta = 0$.

various configurations. Similarly, Fig. 8(b) depicts the negativity for the thermally entangleable set at $\beta = 0$. Note that, even when the initial state is not exactly the one that produces the maximum negativity, one can still obtain an amount of negativity close to the maximum.

VI. ADDITIONAL DISCUSSIONS

A. Generation of entanglement in the presence of dissipation

So far, our discussion revolved around the assumption that any energy-preserving system-bath dynamics is accessible. However, one can also consider the scenario where the system undergoes an open dynamics described by a Lindblad master equation [45–47],

$$\frac{d\rho(t)}{dt} = -i[H, \rho(t)] + \mathcal{L}_t[\rho(t)], \quad (34)$$

where $[\cdot, \cdot]$ denotes the commutator and $\mathcal{L}_t$ is the Lindbladian having the general form

$$\mathcal{L}_t(\rho) = \sum_i r_i(t) \left[L_i(t) \rho L_i(t)^\dagger - \frac{1}{2} \{ L_i(t)^\dagger L_i(t), \rho \} \right], \quad (35)$$

with $\{\cdot, \cdot\}$ denoting the anticommutator, $L_i(t)$ being jump operators, and $r_i(t) \geqslant 0$ being non-negative jump rates. Furthermore, assuming that the quantum system interacts with a large heat bath implies that the system Gibbs state is a stationary solution of the dynamics, $\mathcal{L}_t(\gamma) = 0$ and that the Lindbladian $\mathcal{L}_t$ commutes with the generator of the Hamiltonian dynamics $-i[H, \cdot]$ for all times t.

The dynamics generated by master equations that satisfy two aforementioned properties lead to what is known as a Markovian thermal process, which is known to be a strict subset of thermal operations [48]. The differences between them arise from our degree of control on the bath. Nonetheless,

the entanglement criterion given in Eq. (26) remains valid for Markovian thermal processes. Consequently, we can study the entanglement generation in the presence of dissipation using the same criterion function f.

The additional restriction stemming from the Markovianity of the Lindblad master equations is the most evident when considering the highest excited state $\boldsymbol{p} = (0, 0, 0, 1)$ as the initial state. As analyzed in Sec. V C, the volume of the future thermal cone of entanglement $\mathbf{V}_{\text{TO}}^{\text{ENT}}(\boldsymbol{p})$ defined in Eq. (20) remains maximal for all inverse temperatures β, when we can utilize any thermal operation to generating entanglement. In Fig. 9(a), we present how the volume $\mathbf{V}_{\text{TO}}^{\text{ENT}}(\boldsymbol{p})$ varies as a function of β, when only Markovian thermal processes are allowed. For any β, the volume $\mathbf{V}_{\text{TO}}^{\text{ENT}}(\boldsymbol{p}) > 0$ indicates that the entanglement generation via dissipative dynamics is possible. However, the difference between the entanglement generation via thermal operations is the most pronounced in the high-temperature limit, i.e. when β is small. Furthermore, in the limit $\beta \to \infty$, Markovian thermal processes are as capable as thermal operations for generating entanglement. The detailed behavior of the future thermal cone of entanglement under MTP is depicted in Fig. 9(b).

B. Remarks on higher-dimensional systems

The entanglement structure for multipartite systems with more than two parties is notoriously complex. Multipartite entanglement can be classified using equivalence classes defined with invertible local transformations. Two states are considered to have the same class of entanglement if one can be transformed into the other via LOCC with a nonzero probability [49]. Even in the simplest three-qubit systems, one encounters two distinct classes of entanglement: GHZ-like entanglement and W-like entanglement [49,50], represented
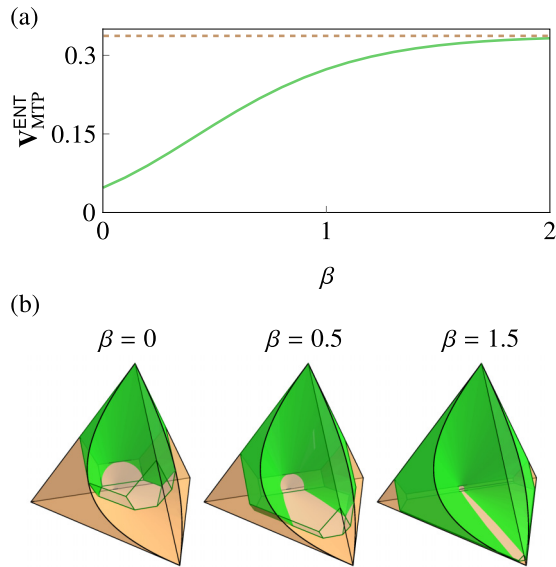
FIG. 9. Entanglement generation via Markovian thermal process. The top plot illustrates the volume of the future thermal cone of entanglement as a function of β for a bipartite system $\rho_{AB} = |11\rangle\langle 11|$ undergoing a Markovian thermal process, depicted by the solid green curve. The dashed orange line represents the volume of the future thermal cone of entanglement for the same state, but under thermal operations. In the bottom plot, the evolution of the Markovian future thermal cone of entanglement (green) with respect to β is shown. Here, the orange shape depicts the future thermal cone under TO, while the internal lighter color with green vertices represents the future cone under MTP.

by the states

$$|\text{GHZ}\rangle = \frac{|000\rangle + |111\rangle}{\sqrt{2}}, \quad |\text{W}\rangle = \frac{|001\rangle + |010\rangle + |100\rangle}{\sqrt{3}}. \tag{36}$$

The n-qubit extensions of two classes exist. In particular, n-qubit GHZ states are defined as

$$|\text{GHZ}_n\rangle = \frac{1}{\sqrt{2}}\left(\underbrace{|0\dots0\rangle}_{n} + \underbrace{|1\dots1\rangle}_{n}\right), \tag{37}$$

an equal superpositions of all n qubits being in the ground state and in the excited state. The concept of W-like entanglement is similarly generalized to n-qubit Dicke states

$$|D_m\rangle = \binom{n}{m}^{-1/2} \sum_{\sigma \in \mathcal{S}_n} P_\sigma \left(\underbrace{|0\dots0\rangle}_{n-m} \otimes \underbrace{|1\dots1\rangle}_{m}\right), \tag{38}$$

where the sum goes over all permutations σ on n elements and P_σ are the respective matricial representations. These states form a basis for the symmetric subspace of an n-qubit system.

Remarkably, different energy level structures give rise to different entanglement structures that can be achieved using thermal operations. Let us assume that the Hamiltonian of the ith qubit is $H_i = E_i|1\rangle\langle 1|$. First, if all the energy gaps are equal, i.e., $E_i = E$, then the n-qubit Hilbert space is divided into energy-degenerate subspaces:

$$\mathcal{H} = \bigoplus_{i=0}^{n} \mathcal{V}_{iE}, \tag{39}$$

each of which spanned by states with a fixed number of excitations i and thus the energy equal to $i \cdot E$. With this energy-level structure, Dicke states $|D_i\rangle$, or W-like entanglement in the three-qubit case, can be generated via thermal operations with nonzero components within the energy-degenerate subspaces.

On the other hand, if we set $E_n = \sum_{i=1}^{n-1} E_i$, we find that the degenerate subspace corresponding to this energy

$$\mathcal{V}_{E_n} = \text{span}\left(|\underbrace{1\dots1}_{n-1}0\rangle, |\underbrace{0\dots0}_{n-1}1\rangle\right) \tag{40}$$

contains states possessing GHZ-like entanglement. Specifically, in the case of three qubits, this configuration leads to GHZ states up to a NOT operation on the third qubit. Similar arguments can be easily extended to systems with larger local dimensions.

Concerning systems with larger local dimensionality, we note that PPT criterion, based on negativity of partial transpose of a state, is a complete entanglement measure not only for two-qubit systems, but also for qubit-qutrit systems as well [42]. In particular, we may consider a system in an energy-incoherent state ρ described by population $\boldsymbol{p} = (p_1, \dots, p_6)$ and subject to local Hamiltonians $H_1 = |1\rangle\langle 1|$ and $H_2 = |1\rangle\langle 1| + 2|2\rangle\langle 2|$. Based on similar arguments as for the qubit-qubit systems, if any of the following two conditions,

$$4\, p_1 \min(p_4, p_5) < (p_2 - p_3)^2,$$
$$4\, p_6 \min(p_2, p_3) < (p_4 - p_5)^2, \tag{41}$$

is satisfied, one of the eigenvalues of the partial transpose ρ^{T_A} can become negative under energy-preserving unitary operations, and therefore, the state is entangleable. Similar expressions can be easily put forward for qubit-qudit systems.

It should be highlighted, however, that in general, complete entanglement measures for multipartite systems beyond 2×2 and 2×3 do not exist, unlike the one based on the PPT criterion, which is effective for two-qubit and two-qutrit cases [41,42], which is reflected in the appearance of so-called bound entanglement [51]. Nevertheless, there exist partial entanglement measures, such as two- and three-tangle for three-qubit systems [52], can be used to provide an outer approximation of the entangleable and nonentangleable sets in such scenarios. Therefore, the geometry of the entangleable set may vary when the entanglement measure is not complete, for instance the aforementioned two- or three-tangle. However, it will be invariant under choice of seemingly different, but complete measures.

VII. OUTLOOK

In this paper, we have investigated the interplay between entanglement and thermodynamics. The minimal thermodynamic assumptions we made, namely that the system bath is closed and evolves via an energy-preserving unitary, constrain

the final entanglement achievable from given initial states. By applying the PPT criterion and constructing future thermal cones, we derived necessary and sufficient conditions for two-qubit initial states that can be transformed into entangled states within thermal operations framework. It turns out that any separable state, apart from a cluster of states around the thermal state, can become entangled. In other words, our investigation demonstrates that entanglement generation is possible, given certain degree of athermality in the initial state. Furthermore, we captured how the entanglement generating capability varies with the ambient temperature, by analyzing the volume of entangleable initial state set, and found that low temperature allows more states to become entangleable. Nevertheless, when the initial state is fixed, we discovered that lowering temperature is not always beneficial and that more detailed considerations on the geometry of thermal cones are needed.

There are several promising avenues for extending and generalizing the results presented in this paper. A concrete and direct generalization consists of using an auxiliary system, a catalyst, to facilitate a process that would not occur spontaneously; see recent reviews [53,54]. The idea of using a catalyst in our context arises from Ref. [55], where the authors demonstrate that catalysis enables the creation of otherwise inaccessible types of correlations by accessing those locked in nondegenerate energy subspaces. As we have discussed, the entanglement generation capacity depends on the structure of degenerate energy subspaces. Employing a catalyst not only increases the number of degenerate energy subspaces but also lift some of the dynamical restrictions imposed by energy conservation. In this regard, the initial steps demonstrating the utility of generating entanglement via thermal operations with the aid of a strict catalyst were presented in Ref. [56]. Furthermore, in Appendix E, we provide an example where correlated catalysis enables the generation of entanglement from an initial state that cannot be entangled without a catalyst. This raises the intriguing question of how one can systematically study the generation of entanglement with the assistance of a catalyst.

In this work, we only considered entanglement generation from initially energy-incoherent states. When we focus on the entanglement generated between degenerate energy levels, coherence between different energy levels cannot contribute. Nevertheless, coherence can still nontrivially affect the entanglement, including those between energy levels with different energy values. Currently, tools and methods available for analyzing coherent state transformations under thermal operations are rather limited [36,57,58]. For two-qubit systems, existing techniques to characterize single-qubit coherent state transformations [36,57] may be adapted to study the entanglement generation. This direction of study will extend our results to the realm where three resources—entanglement, athermality, and coherence–compete and cooperate with each other.

We make a few final remarks on existing literature, to which our work can connect. First, it would be interesting to study the conventional quantifiers of entanglement such as entanglement cost and distillable entanglement [1], which are originally defined via LOCC, and evaluate them with regard to thermodynamic constraints instead. In particular, the gap

between these quantities would then quantify the amount of irreversibility when it comes to the local preparation of entanglement. Lastly, entanglement in continuous-variable (CV) systems is relatively less explored. Extending our analysis to CV systems would be extremely fruitful, considering their widespread use in practical experiments [59] involving optomechanics [60,61], and superconducting setups [62]. For instance, we may use the toolkits developed in the study of Gaussian thermal operations [63] for an analysis similar to what have been done in the current work, and aim to explicate CV entanglement results, such as the recent no-go result [64] for the CV steady-state entanglement generation.

APPENDIX A: FUTURE THERMAL CONE

We briefly review state transition rules under thermal operations and the notion of the future thermal cone, a set of state that can be transformed from a given initial state with thermal operations. First, we introduce thermomajorization relations, which fully characterize the convertibility between two states via thermal operations. The thermomajorization curves, associated to each energy-incoherent state, are defined as the following:

Definition 5 (Thermomajorization curve). Suppose that the Gibbs state $\boldsymbol{\gamma} \in \Delta_d$ with respect to the system Hamiltonian H and the ambient inverse temperature β is given. For each state $\boldsymbol{p} \in \Delta_d$, we define the thermomajorization curve of $\boldsymbol{p}$ as a piecewise-linear function $\mathcal{L}_{\boldsymbol{p}} : [0, 1] \to [0, 1]$ composed of linear segments connecting the point (0,0) and the elbow points $\{(\sum_{i=1}^{k} \gamma_{\pi_{\boldsymbol{p}}^{-1}(i)}, \sum_{i=1}^{k} p_{\pi_{\boldsymbol{p}}^{-1}(i)})\}_{k=1}^{d}$. Here $\pi_{\boldsymbol{p}}$ is the β ordering of $\boldsymbol{p}$, which imposes $p_{\pi_{\boldsymbol{p}}^{-1}(i)}/\gamma_{\pi_{\boldsymbol{p}}^{-1}(i)} \geqslant p_{\pi_{\boldsymbol{p}}^{-1}(j)}/\gamma_{\pi_{\boldsymbol{p}}^{-1}(j)}$ for all $i \leqslant j$.

Note that thermomajorization curves are always concave and nondecreasing by definition. For the Gibbs state $\boldsymbol{\gamma}$, the thermomajorization curve $\mathcal{L}_{\boldsymbol{\gamma}}$ is a straight line from (0,0) to (1,1). From the concavity of the curve and the fact that any $\mathcal{L}_{\boldsymbol{p}}$ passes points (0,0) and (1,1), any thermomajorization curve is above the curve for the Gibbs state. i.e. $\mathcal{L}_{\boldsymbol{p}}(x) \geqslant \mathcal{L}_{\boldsymbol{\gamma}}(x)$ for all $x \in [0, 1]$. See Fig. 10(a) for examples of thermomajorization curves.

Using thermomajorization curves, thermomajorization relations between two states can be established.

Definition 6 (Thermomajorization relation). The thermomajorization relation is a preorder between two energy-incoherent states. If two states $\boldsymbol{p}, \boldsymbol{q} \in \Delta_d$ have corresponding thermomajorization curves $\mathcal{L}_{\boldsymbol{p}}$ and $\mathcal{L}_{\boldsymbol{q}}$, such that
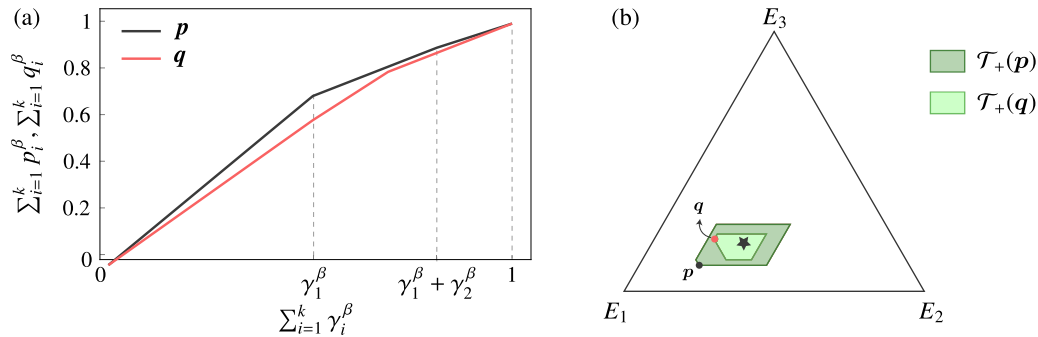
FIG. 10. Thermomajorization and future thermal cone. For two states $p = (0.7, 0.2, 0.1)$ and $q = (0.6, 0.2, 0.2)$ with $\beta = 0.5$, (a) we plot their thermomajorization curves $\mathcal{L}_p(x)$ and $\mathcal{L}_q(x)$, respectively. Since p thermomajorizes q, it implies that one can transform p into q under thermal operations. This can also be observed by examining their (b) future thermal cones, where q lies within the future thermal cone of p. The Gibbs state γ is depicted by a black star $\star$.

$\mathcal{L}_p(x) \geqslant \mathcal{L}_q(x)$ for all $x \in [0, 1]$, we say p thermomajorizes q, or more simply, $p \succ_\beta q$.

Since the thermomajorization relation gives a preorder, not a total order, there exist pairs of states p and q such that neither $p \succ_\beta q$ nor $q \succ_\beta p$ holds. Such pairs are dubbed incomparable. Reamrkably, thermomajorization relations coincide with the state convertibility under thermal operations.

Theorem 2 (Theorem 2 of Ref. [32]). Suppose that $p, q \in \Delta_d$ describe two energy-incoherent states of a system with Hamiltonian H with access to thermal environments with the inverse temperature β. If $p \succ_\beta q$, than p can be transformed to q via some thermal operation.

In particular, the Gibbs state γ is thermomajorized by any other state and thus any state can be converted to the Gibbs state. Conversely, the most excited state with $p = (0, \cdots, 0, 1)$ thermomajorizes all other states in Δ_d and any state can be converted from it.

Theorem 2 provides an efficient way of checking whether a transition from one state to another is feasible. However, it is also possible to characterize the entire set of states that can be attained from an initial state via thermal operations. We refer to such set with an initial state p as the future thermal cone of p and denote it with a symbol $\mathcal{T}_+(p)$.

Lemma 2 (Lemma 12 of Ref. [38]). Suppose $p \in \Delta_d$. The future thermal cone $\mathcal{T}_+(p)$ is a convex polytope with at most $d!$ extreme points each corresponding to permutations $\pi \in \mathcal{S}_d$. The extreme point p^π corresponding to the permutation π can be identified by first constructing its following thermomajorization curve $\mathcal{L}_{p^\pi}$:

(1) The x coordinates of the $\mathcal{L}_{p^\pi}$ elbow points are $x_k = \sum_{i=1}^k \gamma_{\pi^{-1}(i)}$ for $k \in \{1, \dots, d\}$.

(2) The y coordinates of the $\mathcal{L}_{p^\pi}$ elbow points are $y_k = \mathcal{L}_p(x_k)$ for $k \in \{1, \dots, d\}$.

Therefore, $\mathcal{L}_{p^\pi}$ is the piecewise-linear curve that connects $(0,0)$ and elbow points $\{(x_k, y_k)\}_{k=1}^d$, which all lie on the curve $\mathcal{L}_p$.

The thermomajorization relation between the initial state p and extreme states p^π are also known as tight thermomajorization, since all elbow points of $\mathcal{L}_{p^\pi}$ are on the curbe $\mathcal{L}_p$. Furthermore, by construction, each state p^π has the β ordering π. Lemma 2 enables us to characterize the future thermal cone of p by constructing states p^π for each $\pi \in \mathcal{S}_d$, and by taking

their convex hull. Here, we provide the construction of $\mathcal{T}_+(p)$ as a simple corollary of Lemma 2:

Theorem 3 (Future thermal cone). The future thermal cone of a d-dimensional energy-incoherent state p is given by

$$\mathcal{T}_+(p) = \text{conv}[\{p^\pi, \pi \in \mathcal{S}_d\}]. \tag{A1}$$

See Fig. 10(b) for example future thermal cones of two three-level states. In this example, $p \succ_\beta q$ and $\mathcal{T}_+(q) \subset \mathcal{T}_+(p)$; these two relations are indeed equivalent in general. The equivalence directly follows from the transitivity of the preorder $\succ_\beta$, i.e. if $p \succ_\beta q$ and $q \succ_\beta r$, it is always true that $p \succ_\beta r$; hence, $r \in \mathcal{T}_+(q)$ implies $r \in \mathcal{T}_+(p)$.

It is worth mentioning that $\mathcal{T}_+^\beta(p)$ can also be constructed by identifying the entire set of extremal Gibbs-preserving stochastic matrices, as discussed in [38,65,66]. However, if we are only interested in the future thermal cones, following Lemma 2 and Theorem 3 is more efficient.

APPENDIX B: CONVEXITY OF THE SUBSPACE NONENTANGLABLE SET $\mathbb{NE}$

For a bipartite two-qubit state, we now show that the subspace nonentangleable set $\mathbb{NE}$ is convex. The set $\mathbb{NE}$ is defined (in Definition 2) as the set of states satisfying $f(p) \geqslant 0$, where f is a function given in Eq. (27):

$$f(p) = 4p_1(1 - p_1 - p_2 - p_3) - (p_2 - p_3)^2. \tag{B1}$$

To show that the set of states defined by $f(p) \geqslant 0$ is convex, we need to demonstrate that the function f is, counterintuitively, concave. Our task is to verify that for any two arbitrary points $P_1 = (x_1, y_1, z_1)$ and $P_2 = (x_2, y_2, z_2)$, the following condition holds:

$$f[\lambda(x_1, y_1, z_1) + (1 - \lambda)(x_2, y_2, z_3)] \geqslant \lambda f(x_1, y_1, z_1)$$
$$+ (1 - \lambda)f(x_2, y_2, z_2), \tag{B2}$$

for $\lambda \in [0, 1]$. To make the calculation less cumbersome, we can prove convexity by considering two arbitrary boundary points. To do this, we first find the roots of Eq. (B1) with
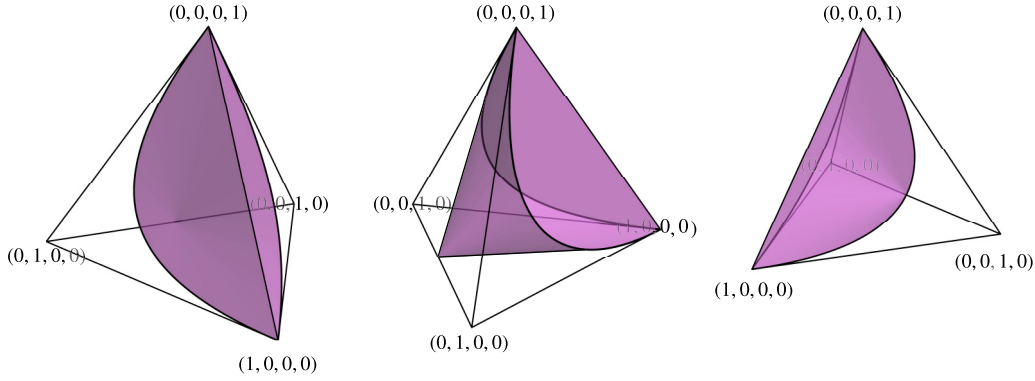
FIG. 11. Subspace nonentangleable set $\mathbb{NE}$. Geometry of the set of qubit-qubit states that cannot get entangled using energy-preserving unitaries. The extreme points of this set include the trivial ones, given by $(1, 0, 0, 0)$, $(0, 0, 0, 1)$, and $(0, 1/2, 1/2, 0)$, as well as a continuous family of boundary points specified by the solution to the quadratic equation $-(p_2 - p_3)^2 + 4p_1(1 - p_1 - p_2 - p_3) = 0$ when solved for p_3.

respect to p_3:

$$
\begin{aligned}
f(p_1, p_2, p_3) = -p_3^2 + 2p_3(p_2 - 2p_1) &- [p_2(4p_1 + p_2) \\
&- 4p_1(1 - p_1)] = 0,
\end{aligned}
\tag{B3}
$$

whose solutions are simply given by

$$
p_3^{(\pm)} = -2p_1 + p_2 \pm 2\sqrt{p_1 - 2p_1 p_2}.
\tag{B4}
$$

By focusing on the boundary conditions, we can simplify the analysis concerning convexity. Specifically, when considering two arbitrary boundary points, the right-hand side of Eq. (B2) is zero. This reduces the problem to verifying whether the left-hand side of this equation is less than or equal to zero. Given that there are two solutions for Eq. (B1), we need to demonstrate that all possible combinations of boundary points $P_i = (x_1, y_1, p_3^{(\pm)})$ for $i\{1, 2\}$, the following inequalities are satisfied:

$$
f[\lambda(x_1, y_1, p_3^{(\pm)}) + (1 - \lambda)(x_2, y_2, p_3^{(\pm)})] \geqslant 0,
\tag{B5}
$$

$$
f[\lambda(x_1, y_1, p_3^{(\pm)}) + (1 - \lambda)(x_2, y_2, p_3^{(\mp)})] \geqslant 0.
\tag{B6}
$$

Furthermore, we must impose the constrain $y_i \leqslant 1/2$ for $i \in \{1, 2\}$ to ensure that the values within the square root in (B4) are real. By rearranging and rewriting the inequalities above, we observe that both inequalities in (B5), as well as inequalities (B6), are equivalent. Consequently, our analysis boils down to demonstrating the validity of the following two inequalities:

$$
\begin{aligned}
4\lambda(1 - \lambda)[x_1(1 - 2y_2) &+ x_2(1 - 2y_1) \\
&\pm 2\sqrt{(x_1 - 2x_1 y_1)(x_2 - 2x_2 y_2)}] \geqslant 0.
\end{aligned}
\tag{B7}
$$

Since the function $4\lambda(1 - \lambda)$ is concave and positive on $\lambda \in [0, 1]$ interval, we only need to prove that the second term is positive. By setting $a = \sqrt{x_1(1 - 2y_2)}$ and $b = \sqrt{x_2(1 - 2y_1)}$ we see that the entire expression is reduced to

$$
4\lambda(1 - \lambda)(a \pm b)^2 \geqslant 0,
\tag{B8}
$$

which completes the proof of concavity of function f.

APPENDIX C: PROOF OF THEOREM 2

We first establish the existence of a subspace entangleable β ordering $(2, 1, 3, 4)$ state for all thermally entangleable states. Yet, the subspace entangleability of the extreme point $\boldsymbol{p}^\star$ is not guaranteed from Lemma 6 yet.

Lemma 7 (Critical β ordering). For any state $\boldsymbol{p} \in \mathbb{TE}$, there exists a state $\boldsymbol{q}$, such that $\boldsymbol{q} \in \mathcal{T}_+^{\text{ENT}}(\boldsymbol{p})$ and the β order $\boldsymbol{\pi_q} = (2, 1, 3, 4)$.

Proof. Suppose that the Lemma is true for all $\boldsymbol{p} \in \mathbb{E}$. Then for any state $\boldsymbol{r} \in \mathbb{TE}$, there exists $\boldsymbol{p} \in \mathbb{E}$ and $\boldsymbol{q} \in \mathcal{T}_+^{\text{ENT}}(\boldsymbol{p}) \subset \mathcal{T}_+^{\text{ENT}}(\boldsymbol{r})$ with $\boldsymbol{\pi_q} = (2, 1, 3, 4)$. Hence, it is sufficient to prove the Lemma for $\boldsymbol{p} \in \mathbb{E}$.

Without loss of generality, assume that $p_2 \geqslant p_3$. From the assumption $\boldsymbol{p} \in \mathbb{E}$, we have $f(\boldsymbol{p}) < 0$ for f defined in Eq. (27). Now, consider another state $\boldsymbol{r}$ such that $\boldsymbol{r} \in \mathcal{T}_+(\boldsymbol{p})$ and

$$
\boldsymbol{r} = \left(p_1 - \delta_1, p_2 + \sum_{i=1,3,4} \delta_i, p_3 - \delta_3, p_4 - \delta_4 \right),
\tag{C1}
$$

for some $\delta_1, \delta_3, \delta_4 \geqslant 0$. We can observe that $f(\boldsymbol{r})$ is decreasing monotonically as $\delta_1, \delta_3, \delta_4$ increases. If $(\boldsymbol{\pi_p})_1 \neq 2$, there always exists a state $\boldsymbol{r}$ in the form of Eq. (C1) and $(\boldsymbol{\pi_r})_1 = 2$. From the monotonicity of $f(\boldsymbol{r})$, this state $\boldsymbol{r} \in \mathcal{T}_+^{\text{ENT}}(\boldsymbol{p})$. We prove the rest of the Lemma by showing there exists $\boldsymbol{q} \in \mathcal{T}_+^{\text{ENT}}(\boldsymbol{r})$ and use $\mathcal{T}_+^{\text{ENT}}(\boldsymbol{r}) \subset \mathcal{T}_+^{\text{ENT}}(\boldsymbol{p})$. Hence, we assume that $(\boldsymbol{\pi_p})_1 = 2$.

Now, suppose that the state $\boldsymbol{p}$ has $p_4 \geqslant p_1 e^{-2\beta E}$. Then a state $\boldsymbol{r}$ such that $r_2 = p_2, r_3 = p_3$, and

$$
r_1 = (1 - e^{-2\beta E})p_1 + p_4, \quad r_4 = e^{-2\beta E}p_1,
\tag{C2}
$$

is in $\mathcal{T}_+(\boldsymbol{p})$ and satisfies $r_1 e^{-2\beta E} \geqslant r_4$. From direct calculation,

$$
f(\boldsymbol{r}) = f(\boldsymbol{p}) - 4(1 - e^{-2\beta E})p_1(p_4 - e^{-2\beta E}p_1) \leqslant f(\boldsymbol{p}),
\tag{C3}
$$

i.e., $\boldsymbol{r} \in \mathcal{T}_+^{\text{ENT}}(\boldsymbol{p})$ whenever $\boldsymbol{p} \in \mathbb{E}$.

Therefore, one can always find $\boldsymbol{q} \in \mathcal{T}_+^{\text{ENT}}(\boldsymbol{p})$ whose β ordering is either (i) $\pi_q = (2, 3, 1, 4)$, (ii) $\pi_q = (2, 1, 4, 3)$, or (iii) $\pi_q = (2, 1, 3, 4)$. We will show that cases (i) and (ii) again

imply the existence of $\boldsymbol{q} \in \mathcal{T}_+^{\text{ENT}}(\boldsymbol{p})$ corresponding to the case (iii), which proves the Lemma.

Case (i): $\pi_{\boldsymbol{p}} = (2, 3, 1, 4)$ with a strict ordering $p_3 > p_1 e^{-\beta E}$. It is always possible to find $\boldsymbol{p}' \in \mathcal{T}_+(\boldsymbol{p})$, such that $\pi_{\boldsymbol{p}'} = (2, 3, 1, 4)$ and $f(\boldsymbol{p}') = 0$ by a convex combination $\boldsymbol{p}' = (1 - \lambda)\boldsymbol{p} + \lambda\boldsymbol{\gamma}$, where $\lambda \in [0, 1]$ and γ is the Gibbs state. Now assume that $\boldsymbol{q} \in \mathcal{T}_+(\boldsymbol{p}')$ is a state with $\pi_{\boldsymbol{q}} = (2, 1, 3, 4)$ and

$$\boldsymbol{q} = (p_1' + \delta, p_2', p_3' - \delta, p_4'), \tag{C4}$$

with some $\delta > 0$. Such a state always exists since $p_3' > p_1' e^{-\beta E}$. The entanglement witness gives

$$f(\boldsymbol{q}) = 4(p_1' + \delta)(p_4') - (p_2' - p_3' + \delta)^2$$
$$= -\delta^2 + 2(p_3' + 2p_4' - p_2')\delta, \tag{C5}$$

where we used $f(\boldsymbol{p}') = 0$ for the second equality. If $p_1' = 0$, we have $p_4' = 0$ from the β order of $\boldsymbol{p}'$ and $p_2' = p_3'$ from $f(\boldsymbol{p}') = 0$; hence, $f(\boldsymbol{q}) < 0$. When $p_1' \neq 0$, we use $p_4' = (p_2' - p_3')^2/(4p_1')$ to get

$$f(\boldsymbol{q}) = -\delta^2 - 2(p_2' - p_3')\left(1 - \frac{p_2' - p_3'}{2p_1'}\right)\delta. \tag{C6}$$

Recall $4(p_1')^2 \geqslant 4p_1'p_4' = (p_2' - p_3')^2$ implying $1 - \frac{p_2' - p_3'}{2p_1'} \geqslant 0$ and thus $f(\boldsymbol{q}) < 0$.

Case (ii): $\pi_{\boldsymbol{p}} = (2, 1, 4, 3)$. There exists $\boldsymbol{p}' \in \mathcal{T}_+(\boldsymbol{p})$, such that $\pi_{\boldsymbol{p}'} = (2, 1, 4, 3)$ and $f(\boldsymbol{p}') = 0$ and also $\boldsymbol{q} \in \mathcal{T}_+(\boldsymbol{p}')$, such that

$$\boldsymbol{q} = (p_1', p_2', p_3' + \delta, p_4' - \delta), \tag{C7}$$

with $\pi_{\boldsymbol{q}} = (2, 1, 3, 4)$. Observe that

$$f(\boldsymbol{q}) = 4(p_1')(p_4' - \delta) - (p_2' - p_3' - \delta)^2$$
$$= -\delta^2 - 2(2p_1' - p_2' + p_3')\delta < 0 \tag{C8}$$

for any $\delta > 0$. ∎

Now we use geometric arguments to prove the remaining part of Theorem 1. To do this, we define generalized boundary sets.

Definition 7 (d-dimensional boundaries). Let X be a convex set and $C_d(X)$ be a set of all $(d + 1)$-dimensional convex subsets $Y \subset X$. d-dimensional boundary of X is defined as

$$\text{Bd}_d(X) := \{x \mid \nexists Y \in C_d(X), \text{ such that } x \in \text{int}(Y)\}. \tag{C9}$$

Intuitively, $\text{Bd}_d(X)$ cannot be written as a convex combination of $d + 2$ extreme points of X with nonzero weights; hence, $\text{Bd}_0(X)$ is a set of extreme points of X, while $\text{Bd}_1(X)$ is a set of points of the edges of X. Furthermore, if X is D dimensional, $\text{Bd}_{D-1}(X)$ reduces to the conventional boundary, ∂X

Note that $\text{Bd}_d(X) \subset \text{Bd}_{d+1}(X)$ for any $d \geqslant 0$: if it is impossible write a state x as a convex combination of any $d + 2$ extreme points, it is also impossible to write it as a convex combination of any $d + 3$ extreme points. Using this definition, we establish a helpful proposition.

Proposition 8 (Intersection of d-dimensional boundaries). Suppose that a convex set A is a subset of a convex set B and their boundaries intersect, i.e., $A \subset B$ and $\partial A \cap \partial B \neq \emptyset$. Then, for all d-dimensional boundaries,

$$A \cap \text{Bd}_d(B) \subset \text{Bd}_d(A). \tag{C10}$$

If we have additional condition $[\text{Bd}_d(A) \setminus \text{Bd}_{d-1}(A)] \cap \text{Bd}_d(B) = \emptyset$, for some d, we find

$$A \cap \text{Bd}_d(B) \subset \text{Bd}_{d-1}(A). \tag{C11}$$

Proof. For the first part of the proposition, suppose that there exists a point $x \notin \text{Bd}_d(A)$ such that $x \in A \cap \text{Bd}_d(B)$. Then there exists a convex subset Y of A having $d + 2$ extreme points and containing x in $\text{int}(Y)$. Yet, this set Y is also a convex subset of B having the same property, which contradicts $x \in A \cap \text{Bd}_d(B)$. The second part of the proposition follows directly from combining Eq. (C10) and the additional assumption $[\text{Bd}_d(A) \setminus \text{Bd}_{d-1}(A)] \cap \text{Bd}_d(B) = \emptyset$. ∎

Now we proceed to prove Theorem 1, which states that $\boldsymbol{p}^\star \in \mathbb{E}$ whenever $\boldsymbol{p} \in \mathbb{TE}$. First, consider mixtures of the initial state $\boldsymbol{p}$ and the Gibbs state $\boldsymbol{\gamma}$ that can be written as $\boldsymbol{p}^{(x)} = (1 - x)\boldsymbol{p} + x\boldsymbol{\gamma}$ for some $x \in [0, 1]$. Future thermal cones between these states have a hierarchy $\mathcal{T}_+(\boldsymbol{p}^{(y)}) \subset \mathcal{T}_+(\boldsymbol{p}^{(x)})$ whenever $y \geqslant x$. Then there exists a coefficient $a \in (0, 1)$, such that

$$\mathcal{T}_+(\boldsymbol{p}^{(a)}) \subset \mathbb{NE}, \quad \partial[\mathcal{T}_+(\boldsymbol{p}^{(a)})] \cap \partial(\mathbb{NE}) \neq \emptyset, \tag{C12}$$

since $\mathcal{T}_+(\boldsymbol{p}) \not\subset \mathbb{NE}$, while $\mathcal{T}_+(\boldsymbol{\gamma}) \subset \text{int}(\mathbb{NE})$. The Gibbs state $\boldsymbol{\gamma}$ is always full rank and so is $\boldsymbol{p}^{(a)}$, i.e., $\boldsymbol{p}^{(a)} \in \text{int}(\Delta_4)$ and $\mathcal{T}_+(\boldsymbol{p}) \subset \text{int}(\Delta_4)$.

Now we show that $\{\text{Bd}_1[\mathcal{T}_+(\boldsymbol{p}^{(a)})] \setminus \text{Bd}_0[\mathcal{T}_+(\boldsymbol{p}^{(a)})]\} \cap \partial(\mathbb{NE}) = \emptyset$. Let $\boldsymbol{q}$ be a state on the edge of $\mathcal{T}_+(\boldsymbol{p}^{(a)})$ but not on the vertex of it, i.e. $\boldsymbol{q} \in \{\text{Bd}_1[\mathcal{T}_+(\boldsymbol{p}^{(a)})] \setminus \text{Bd}_0[\mathcal{T}_+(\boldsymbol{p}^{(a)})]\}$. Since $\mathbb{NE}$ is convex, if $\boldsymbol{q} \in \partial(\mathbb{NE})$, the entire edge containing $\boldsymbol{q}$ should be included within $\partial(\mathbb{NE})$. Recall that $\mathcal{T}_+(\boldsymbol{p}^{(a)})$ is a polyhedron whose edges are defined as segments of lines on which two of the populations are fixed, e.g. $\boldsymbol{q} = (p_1^{(a)}, p_2^{(a)}, t, 1 - p_1^{(a)} - p_2^{(a)} - t)$ and for some $t \in (t_1, t_2)$. Then the entire edge can be written as a set of states

$$\left\{\left(p_1^{(a)}, p_2^{(a)}, t, 1 - p_1^{(a)} - p_2^{(a)} - t\right) \mid t \in [t_1, t_2]\right\} \subset \partial(\mathbb{NE}). \tag{C13}$$

Yet, it is impossible to satisfy $f(p_1^{(a)}, p_2^{(a)}, t, 1 - p_1^{(a)} - p_2^{(a)} - t) = 0$ for a finite range $t \in [t_1, t_2]$, which contradicts Eq. (C13). The same can be proven for any two fixed populations. Likewise, $[\text{Bd}_2(\mathcal{T}_+(\boldsymbol{p}^{(a)})) \setminus \text{Bd}_1(\mathcal{T}_+(\boldsymbol{p}^{(a)}))] \cap \partial(\mathbb{NE}) = \emptyset$: if any point on $[\text{Bd}_2(\mathcal{T}_+(\boldsymbol{p}^{(a)})) \setminus \text{Bd}_1(\mathcal{T}_+(\boldsymbol{p}^{(a)}))]$ is included in $\partial(\mathbb{NE})$, at least one entire edge of $\mathcal{T}_+(\boldsymbol{p}^{(a)})$ should also be included, which is not possible.

Using Proposition 7 twice with $A = \mathcal{T}_+(\boldsymbol{p}^{(a)})$ and $B = \mathbb{NE}$, we have

$$\mathcal{T}_+(\boldsymbol{p}^{(a)}) \cap \partial(\mathbb{NE}) = \mathcal{T}_+(\boldsymbol{p}^{(a)}) \cap \partial(\mathbb{NE}) \subset \text{Bd}_0[\mathcal{T}_+(\boldsymbol{p}^{(a)})], \tag{C14}$$

i.e., only extreme points of $\mathcal{T}_+(\boldsymbol{p}^{(a)})$ can be included in the set $\partial(\mathbb{NE})$.

We finally use Lemma 6. Since $\boldsymbol{p}^{(a)} \in \partial(\mathbb{TE})$, there must exist $\boldsymbol{q} \in \mathcal{T}_+(\boldsymbol{p}^{(a)})$ with β-ordering $(2, 1, 3, 4)$ that is in $\partial(\mathbb{E}) = \partial(\mathbb{NE})$. However, only extreme points of $\mathcal{T}_+(\boldsymbol{p}^{(a)})$ can be in $\partial(\mathbb{NE})$, implying that the $(2, 1, 3, 4)$ extreme point

$$(1 - a)\boldsymbol{p}^\star + a\boldsymbol{\gamma} \in \partial(\mathbb{NE}). \tag{C15}$$

From $\boldsymbol{\gamma} \in \text{int}(\mathbb{NE})$, we obtain $\boldsymbol{p}^\star \in \mathbb{E}$, which concludes the proof.

APPENDIX D: THERMAL INITIAL STATES

In this section, we derive the critical temperatures above or below which the initially thermal state become entangleable. We denote the inverse temperature of the system as β_S and that of the environment as β. To simplify the notation, we use Boltzmann weights $\Delta_S := e^{-\beta_S E}$, $\Delta := e^{-\beta E}$,, and partition functions $Z_S := (1 + \Delta_S)^2$, $Z := (1 + \Delta)^2$. Then the initial state can be written as

$$p = \frac{1}{Z_S}\left(1, \Delta_S, \Delta_S, \Delta_S^2\right). \tag{D1}$$

When $\beta_S > \beta$, i.e. when the system is cooler than the environment, the β ordering of p is (1, 2, 3, 4). The extreme point $p^\star$ of $\mathcal{T}_+(p)$, corresponding to the ordering $\pi^\star = (2, 1, 3, 4)$ can be easily obtained by maximally exchanging populations (referred to as the β-swapping in Refs. [28,38,67]) between first two levels $|00\rangle$ and $|01\rangle$,

$$p^\star = \frac{1}{Z_S}\left(1 - \Delta + \Delta_S, \Delta, \Delta_S, \Delta_S^2\right). \tag{D2}$$

We want the entanglement measure to be negative, i.e.,

$$f(p^\star) = \frac{1}{Z_S^2}\left\{4\Delta_S^2[1 - (\Delta - \Delta_S)] - (\Delta - \Delta_S)^2\right\} < 0. \tag{D3}$$

Solving this inequality, we obtain

$$\Delta > \Delta_{C_1} := \Delta_S\left(1 + 2\sqrt{1 + \Delta_S^2} - 2\Delta_S\right), \tag{D4}$$

equivalent to Eq. (29) in Sec. V B.

When the system temperature is low, that is, when $\Delta_S \ll 1$, Eq. (D4) can be written with the Taylor expansion

$$\Delta_{C_1} = 3\Delta_S + O\left(\Delta_S^2\right), \tag{D5}$$

yielding the approximation $\beta_{C_1} E \simeq \beta_S E - \log 3$, up to the leading order.

Now, consider the other case where $\beta_S < \beta$; the system is now hotter than the surrounding environment, and the β order of the initial state $\mathbf{p}$ is now (4, 3, 2, 1). Thermomajorization relations reveal that the extreme point $p^\star$ now has two distinct forms depending on the environment temperature β. If $1 > \Delta + \Delta^2$, that is, $\beta E \geqslant -\log[\frac{\sqrt{5}-1}{2}]$, the extreme state is

$$p^\star = \frac{1}{Z_S}\{1 + (\Delta_S - \Delta)(1 + \Delta), \Delta_S(1 + \Delta_S - \Delta), \Delta, \Delta^2\}. \tag{D6}$$

On the other hand, when $\beta E < -\log[\frac{\sqrt{5}-1}{2}]$,

$$p^\star = \frac{1}{Z_S}\left(\frac{\Delta_S}{\Delta}, \Delta_S(1 + \Delta_S - \Delta), 1 + \Delta_S + \Delta_S\Delta - \Delta \right.$$
$$\left. -\frac{\Delta_S}{\Delta}, \Delta^2\right). \tag{D7}$$

For the latter case Eq. (D7), the entanglement measure is evaluated as

$$f(p^\star) = \frac{1}{Z_S^2\Delta^2}\{4\Delta_S\Delta^3 - (\Delta_S - \Delta)^2[1 + \Delta(\Delta_S - \Delta)]^2)\}. \tag{D8}$$

However, in the range where Eq. (D7) is valid, $1 \geqslant \Delta_S > \Delta > \frac{\sqrt{5}-1}{2}$, entanglement measure is always positive and there is no critical inverse temperature β_{C_2}. For the former case Eq. (D6) with $1 \geqslant \Delta_S > \Delta$ and $\frac{\sqrt{5}-1}{2} \geqslant \Delta > 0$,

$$f(p^\star) = \frac{1}{Z_S^2}\{-(\Delta_S - \Delta)^2(1 + \Delta_S)^2$$
$$+ 4\Delta^2[1 + \Delta_S - (1 - \Delta_S)\Delta + \Delta^2]\} \tag{D9}$$

and the solution for $f(p^\star) = 0$ can be obtained by solving this quartic equation. Unfortunately, there is no simple explicit solution for this equation. To approximate the critical value, let us assume that $\Delta_S \ll 1$, i.e. $\beta_S E \gg 1$. Ignoring the Z_S factor in Eq. (D9) and taking only the leading-order terms of Δ and Δ_S, we get the approximation

$$Z_S^2 f(p^\star) = 3\Delta^2 + 2\Delta\Delta_S - \Delta_S^2 + O\left(\Delta_S^3\right), \tag{D10}$$

and the solution of $f(p^\star) = 0$ is approximately $\Delta \simeq \frac{\Delta_S}{3}$. In other words, $\beta_{C_2} E \simeq \beta_S E + \log 3$.

APPENDIX E: CATALYTIC ADVANTAGES ON ENTANGLEMENT GENERATION: A TOY EXAMPLE

We now construct a simple toy example to demonstrate that if a catalyst is allowed, entanglement can be generated from states that cannot achieve this under thermal operations without a catalyst. For simplicity, we assume $\beta = 0$ and consider a bipartite state

$$\rho_{AB} = \frac{2}{5}|00\rangle\langle00| + \frac{1}{4}|01\rangle\langle01| + \frac{33}{100}|10\rangle\langle10| + \frac{1}{50}|11\rangle\langle11|, \tag{E1}$$

with local Hamiltonians $H_X = |1\rangle\langle1|$ for $X \in \{A, B\}$. The initial bipartite state ρ_{AB} belongs to the thermally nonentangleable set, i.e., $p = \text{eig}(\rho) \in \mathbb{TNE}$. Hence, at $\beta = 0$, there is no thermal operation capable of entangling ρ_{AB}.

Let us now consider a two-dimensional catalyst, prepared in a state

$$\omega_C = \frac{73}{100}|0\rangle\langle0| + \frac{27}{100}|1\rangle\langle1|, \tag{E2}$$

and described described by a Hamiltonian $H_C = |1\rangle\langle1|$, such that the joint Hamiltonian of the composite system ABC is given by

$$H_{ABC} = \begin{pmatrix} 0 & 0 & 0 & 0 & 0 & 0 & 0 & 0 \\ 0 & 1 & 0 & 0 & 0 & 0 & 0 & 0 \\ 0 & 0 & 1 & 0 & 0 & 0 & 0 & 0 \\ 0 & 0 & 0 & 1 & 0 & 0 & 0 & 0 \\ 0 & 0 & 0 & 0 & 2 & 0 & 0 & 0 \\ 0 & 0 & 0 & 0 & 0 & 2 & 0 & 0 \\ 0 & 0 & 0 & 0 & 0 & 0 & 2 & 0 \\ 0 & 0 & 0 & 0 & 0 & 0 & 0 & 3 \end{pmatrix}. \tag{E3}$$

where the colors in each block highlight the degenerate energy subspaces. We assume that the total system

evolves according to the following energy-preserving unitary transformation

$$U = \begin{pmatrix} 1 & 0 & 0 & 0 & 0 & 0 & 0 & 0 \\ 0 & 1 & 0 & 0 & 0 & 0 & 0 & 0 \\ 0 & 0 & 0 & 1 & 0 & 0 & 0 & 0 \\ 0 & 0 & 1 & 0 & 0 & 0 & 0 & 0 \\ 0 & 0 & 0 & 0 & 0 & 1 & 0 & 0 \\ 0 & 0 & 0 & 0 & 0 & 0 & 1 & 0 \\ 0 & 0 & 0 & 0 & 1 & 0 & 0 & 0 \\ 0 & 0 & 0 & 0 & 0 & 0 & 0 & 1 \end{pmatrix}, \tag{E4}$$

which maps the composite system to $\sigma_{ABC} := U(\rho_{AB} \otimes \omega_C)U^\dagger$, where the reduced states of AB become

$$\sigma_{AB} = \frac{949}{2000}|00\rangle\langle00| + \frac{613}{5000}|01\rangle\langle01| + \frac{771}{2500}|10\rangle\langle10|$$

$$+ \frac{189}{2000}|11\rangle\langle11| \tag{E5}$$

while the catalyst returns exactly to the same state as it started $\sigma_C = \omega_C$.

Therefore, one can easily verify that the final state no longer belongs to $\mathbb{TNE}$, i.e., $\boldsymbol{q} := \mathrm{eig}(\sigma) \notin \mathbb{TNE}$. This implies that a thermal operation capable of mapping σ_{AB} into an entangled state can be constructed.

[1] R. Horodecki, P. Horodecki, M. Horodecki, and K. Horodecki, Quantum entanglement, Rev. Mod. Phys. **81**, 865 (2009).

[2] R. Kosloff, Quantum thermodynamics: A dynamical viewpoint, Entropy **15**, 2100 (2013).

[3] J. Goold, M. Huber, A. Riera, L. del Rio, and P. Skrzypczyk, The role of quantum information in thermodynamics—a topical review, J. Phys. A: Math. Theor. **49**, 143001 (2016).

[4] S. Vinjanampathy and J. Anders, Quantum thermodynamics, Contemp. Phys. **57**, 545 (2016).

[5] S. Deffner and S. Campbell, *Quantum Thermodynamics: An Introduction to the Thermodynamics of Quantum Information* (Morgan & Claypool, Melbourne, 2019)

[6] J. Oppenheim, M. Horodecki, P. Horodecki, and R. Horodecki, Thermodynamical approach to quantifying quantum correlations, Phys. Rev. Lett. **89**, 180402 (2002).

[7] K. V. Hovhannisyan, M. Perarnau-Llobet, M. Huber, and A. Acín, Entanglement generation is not necessary for optimal work extraction, Phys. Rev. Lett. **111**, 240401 (2013).

[8] M. Huber, M. Perarnau-Llobet, K. V. Hovhannisyan, P. Skrzypczyk, C. Klöckl, N. Brunner, and A. Acín, Thermodynamic cost of creating correlations, New J. Phys. **17**, 065008 (2015).

[9] M. Perarnau-Llobet, K. V. Hovhannisyan, M. Huber, P. Skrzypczyk, N. Brunner, and A. Acín, Extractable work from correlations, Phys. Rev. X **5**, 041011 (2015).

[10] R. Alicki and M. Fannes, Entanglement boost for extractable work from ensembles of quantum batteries, Phys. Rev. E **87**, 042123 (2013).

[11] F. Verstraete, K. Audenaert, and B. De Moor, Maximally entangled mixed states of two qubits, Phys. Rev. A **64**, 012316 (2001).

[12] N. Friis, M. Huber, and M. Perarnau-Llobet, Energetics of correlations in interacting systems, Phys. Rev. E **93**, 042135 (2016).

[13] S. Ishizaka and T. Hiroshima, Maximally entangled mixed states under nonlocal unitary operations in two qubits, Phys. Rev. A **62**, 022310 (2000).

[14] M. S. Kim, Jinhyoung Lee, D. Ahn, and P. L. Knight, Entanglement induced by a single-mode heat environment, Phys. Rev. A **65**, 040101(R) (2002).

[15] M. B. Plenio and S. F. Huelga, Entangled light from white noise, Phys. Rev. Lett. **88**, 197901 (2002).

[16] L. Hartmann, W. Dür, and H.-J. Briegel, Steady-state entanglement in open and noisy quantum systems, Phys. Rev. A **74**, 052304 (2006).

[17] L. Hartmann, W. Dür, and H. Briegel, Entanglement and its dynamics in open, dissipative systems, New J. Phys. **9**, 230 (2007).

[18] B. Bellomo and M. Antezza, Steady entanglement out of thermal equilibrium, Europhys. Lett. **104**, 10006 (2013).

[19] J. B. Brask, G. Haack, N. Brunner, and M. Huber, Autonomous quantum thermal machine for generating steady-state entanglement, New J. Phys. **17**, 113029 (2015).

[20] S. Khandelwal, B. Annby-Andersson, G. F. Diotallevi, A. Wacker, and A. Tavakoli, Maximal steady-state entanglement in autonomous quantum thermal machines, arXiv:2401.01776.

[21] G. Gour, M. P. Müller, V. Narasimhachar, R. W. Spekkens, and N. Yunger Halpern, The resource theory of informational nonequilibrium in thermodynamics, Phys. Rep. **583**, 1 (2015).

[22] F. G. S. L. Brandão, M. Horodecki, J. Oppenheim, J. M. Renes, and R. W. Spekkens, Resource theory of quantum states out of thermal equilibrium, Phys. Rev. Lett. **111**, 250404 (2013).

[23] D. Janzing, P. Wocjan, R. Zeier, R. Geiss, and T. Beth, Thermodynamic cost of reliability and low temperatures: Tightening Landauer's principle and the second law, Int. J. Theor. Phys. **39**, 2717 (2000).

[24] M. Horodecki and J. Oppenheim, (Quantumness in the context of) resource theories, Int. J. Mod. Phys. B **27**, 1345019 (2013).

[25] F. G. S. L. Brandão, M. Horodecki, N. H. Y. Ng, J. Oppenheim, and S. Wehner, The second laws of quantum thermodynamics, Proc. Natl. Acad. Sci. USA **112**, 3275 (2015).

[26] M. Lostaglio, An introductory review of the resource theory approach to thermodynamics, Rep. Prog. Phys. **82**, 114001 (2019).

[27] C. Sparaciari, M. Goihl, P. Boes, J. Eisert, and N. H. Y. Ng, Bounding the resources for thermalizing many-body localized systems, Commun. Phys. **4**, 3 (2021).

[28] J. Czartowski, A. de Oliveira Junior, and K. Korzekwa, Thermal recall: Memory-assisted Markovian thermal processes, PRX Quantum **4**, 040304 (2023).

[29] J. Son and N. H. Y. Ng, A hierarchy of thermal processes collapses under catalysis, arXiv:2303.13020.

[30] Á. M. Alhambra, M. Lostaglio, and C. Perry, Heat-bath algorithmic cooling with optimal thermalization strategies, Quantum **3**, 188 (2019).

[31] G. Torun, O. Pusuluk, and Ö. E. Müstecaplıoğlu, A compendious review of majorization-based resource theories: Quantum information and quantum thermodynamics, Turk. J. Phys. **47**, 141 (2023).

[32] M. Horodecki and J. Oppenheim, Fundamental limitations for quantum and nanoscale thermodynamics, Nat. Commun. **4**, 2059 (2013).

[33] E. T. Jaynes and F. W. Cummings, Comparison of quantum and semiclassical radiation theories with application to the beam maser, Proc. IEEE **51**, 89 (1963).

[34] J. I. Cirac and P. Zoller, Preparation of macroscopic superpositions in many-atom systems, Phys. Rev. A **50**, R2799 (1994).

[35] G. Vidal and R. F. Werner, Computable measure of entanglement, Phys. Rev. A **65**, 032314 (2002).

[36] K. Korzekwa, Structure of the thermodynamic arrow of time in classical and quantum theories, Phys. Rev. A **95**, 052318 (2017).

[37] A. de Oliveira Junior, J. Czartowski, K. Życzkowski, and K. Korzekwa, Geometric structure of thermal cones, Phys. Rev. E **106**, 064109 (2022).

[38] M. Lostaglio, Á. M. Alhambra, and C. Perry, Elementary thermal operations, Quantum **2**, 52 (2018).

[39] D. J. Lostaglio and T. Rudolph, Description of quantum coherence in thermodynamic processes requires constraints beyond free energy, Nat. Commun. **6**, 6383 (2015).

[40] J. O. Faist and R. Renner, Gibbs-preserving maps outperform thermal operations in the quantum regime, New J. Phys. **17**, 043003 (2015).

[41] A. Peres, Separability criterion for density matrices, Phys. Rev. Lett. **77**, 1413 (1996).

[42] M. Horodecki, P. Horodecki, and R. Horodecki, Separability of mixed states: Necessary and sufficient conditions, Phys. Lett. A **223**, 1 (1996).

[43] M. Horodecki, P. Horodecki, and R. Horodecki, Mixed-state entanglement and distillation: Is there a "bound" entanglement in nature? Phys. Rev. Lett. **80**, 5239 (1998).

[44] L. Chen, Y. Yang, and W.-S. Tang, Schmidt number of bipartite and multipartite states under local projections, Quantum Inf. Process. **16**, 75 (2017).

[45] A. Kossakowski, On quantum statistical mechanics of non-Hamiltonian systems, Rep. Math. Phys. **3**, 247 (1972).

[46] V. Gorini, A. Kossakowski, and E. C. G. Sudarshan, Completely positive dynamical semigroups of *N*-level systems, J. Math. Phys. **17**, 821 (1976).

[47] G. Lindblad, On the generators of quantum dynamical semigroups, Commun. Math. Phys. **48**, 119 (1976).

[48] M. Lostaglio and K. Korzekwa, Continuous thermomajorization and a complete set of laws for Markovian thermal processes, Phys. Rev. A **106**, 012426 (2022).

[49] W. Dür, G. Vidal, and J. I. Cirac, Three qubits can be entangled in two inequivalent ways, Phys. Rev. A **62**, 062314 (2000).

[50] A. Acín, D. Bruß, M. Lewenstein, and A. Sanpera, Classification of mixed three-qubit states, Phys. Rev. Lett. **87**, 040401 (2001).

[51] M. Gaida and M. Kleinmann, Seven definitions of bipartite bound entanglement, J. Phys. A: Math. Theor. **56**, 385302 (2023).

[52] V. Coffman, J. Kundu, and W. K. Wootters, Distributed entanglement, Phys. Rev. A **61**, 052306 (2000).

[53] C. Datta, T. V. Kondra, M. Miller, and A. Streltsov, Catalysis of entanglement and other quantum resources, Rep. Prog. Phys. **86**, 116002 (2023).

[54] P. Lipka-Bartosik, H. Wilming, and N. H. Y. Ng, Catalysis in quantum information theory, arXiv:2306.00798.

[55] P. Lipka-Bartosik, G. F. Diotallevi, and P. Bakhshinezhad, Fundamental limits on anomalous energy flows in correlated quantum systems, Phys. Rev. Lett. **132**, 140402 (2024).

[56] J. Czartowski and A. de Oliveira Junior, Catalytic transformations for thermal operations, Phys. Rev. Res. **6**, 033203 (2024).

[57] M. Lostaglio, K. Korzekwa, D. Jennings, and T. Rudolph, Quantum coherence, time-translation symmetry, and thermodynamics, Phys. Rev. X **5**, 021001 (2015).

[58] G. Gour, D. Jennings, F. Buscemi, R. Duan, and I. Marvian, Quantum majorization and a complete set of entropic conditions for quantum thermodynamics, Nat. Commun. **9**, 5352 (2018).

[59] U. Andersen, G. Leuchs, and C. Silberhorn, Continuous-variable quantum information processing, Laser Photon. Rev. **4**, 337 (2010).

[60] T. Rocheleau, T. Ndukum, C. Macklin, J. B. Hertzberg, A. A. Clerk, and K. C. Schwab, Preparation and detection of a mechanical resonator near the ground state of motion, Nature (London) **463**, 72 (2010).

[61] J. D. Teufel, T. Donner, D. Li, J. W. Harlow, M. S. Allman, K. Cicak, A. J. Sirois, J. D. Whittaker, K. W. Lehnert, and R. W. Simmonds, Sideband cooling of micromechanical motion to the quantum ground state, Nature (London) **475**, 359 (2011).

[62] F. Reiter, L. Tornberg, G. Johansson, and A. S. Sørensen, Steady-state entanglement of two superconducting qubits engineered by dissipation, Phys. Rev. A **88**, 032317 (2013).

[63] A. Serafini, M. Lostaglio, S. Longden, U. Shackerley-Bennett, C.-Y. Hsieh, and G. Adesso, Gaussian thermal operations and the limits of algorithmic cooling, Phys. Rev. Lett. **124**, 010602 (2020).

[64] B. Longstaff, M. G. Jabbour, and J. B. Brask, Impossibility of bosonic autonomous entanglement engines in the weak-coupling limit, Phys. Rev. A **108**, 032209 (2023).

[65] P. Mazurek and M. Horodecki, Decomposability and convex structure of thermal processes, New J. Phys. **20**, 053040 (2018).

[66] P. Mazurek, Thermal processes and state achievability, Phys. Rev. A **99**, 042110 (2019).

[67] J. Son and N. H. Y. Ng, Catalysis in action via elementary thermal operations, New J. Phys. **26**, 033029 (2024).